Contents lists available at ScienceDirect

Chemical Engineering Research and Design

journal homepage: www.elsevier.com/locate/cherd

Process intensification in multicomponent distillation: A review of recent advancements

*Zheyu Jiang, Rakesh Agrawal**

Davidson School of Chemical Engineering, Purdue University, West Lafayette, IN 47907, USA

ARTICLE INFO

Article history:
Received 10 December 2018
Received in revised form 12 April 2019
Accepted 15 April 2019
Available online 22 April 2019

Keywords:
Process intensification
Multicomponent distillation
Separation

ABSTRACT

Process intensification (PI) is an emerging concept in chemical engineering that describes the design innovations that lead to significant shrinkage in size and boost in efficiency of a process plant. Distillation, the most commonly used separation technique in the chemical industry, is a crucial component of PI. Here, we systematically discuss the following aspects of PI in non-azeotropic multicomponent distillation: (1) Introducing thermal couplings to eliminate intermediate reboilers and condensers to save energy and capital cost; (2) Improving operability of thermally coupled columns by means of eliminating vapor streams in thermal couplings with only liquid transfers or column section rearrangement; (3) Enabling double and multi-effect distillation of thermally coupled configurations to further reduce heat duty; (4) Performing simultaneous heat and mass integration among thermally coupled columns to reduce the number of columns and heat duty; and (5) Conducting any thermally coupled distillation in n-product streams using 1 to $n-2$ column shells with operable novel dividing wall columns. We demonstrate these aspects of PI through examples to illustrate how they lead to compact, easy-to-operate, energy efficient and cost effective multicomponent distillation system designs.

Nomenclature

PI	process intensification
CTC	completely thermally coupled
TC	thermally coupled
FTC	fully thermally coupled
ALT	Agrawal's liquid transfer
HMI	heat and mass integration
HMA	heat and mass integration with additional section
HMP	HMA between final product ends for CTC configurations
DWC	dividing wall column
MTA method	Madenoor Ramapriya, Tawarmalani, and Agrawal method
AMR dividing wall	Agrawal and Madenoor Ramapriya dividing wall

1. Introduction

Distillation accounts for 90–95% of all separations and consumes 40–60% of energy in the chemical and refining industries (Humphrey, 1992; Sholl and Lively, 2016). It deals with some of world's largest and most profitable separations, such as crude oil fractionation, hydrocarbon separation from steam cracking, and natural gas liquids (NGL) separation. To distill a non-azeotropic multicomponent mixture that contains n components into n product streams, each enriched in one of the components, a sequence of distillation columns known as a distillation configuration is required. To identify any attractive distillation configuration for a given separation task, it is important to first define the appropriate search space that contains, and only contains, all useful configurations. Distillation configurations can be categorized in many ways. One way is based on splits, the smallest unit in a distillation configuration that represents the separation of a mixture into two product streams. Sharp splits produce top and bottom product streams with no overlapping components, whereas non-sharp splits produce product streams with a non-negligible number of overlapping components. Accordingly, distillation configu-

* *Corresponding author.*
E-mail address: agrawalr@purdue.edu (R. Agrawal).
https://doi.org/10.1016/j.cherd.2019.04.023

rations can be classified as either *sharp split configurations*, if all their splits are sharp, or *non-sharp split configurations*, if at least one split is non-sharp (Giridhar and Agrawal, 2010a). On the next level, distillation configurations can also be classified by the number of columns used, namely *regular-column* (using exactly $n-1$ columns), *sub-column* (using $<n-1$ columns), and *plus-column* (using $>n-1$ columns) *configurations* (Shah and Agrawal, 2010). Systematic analyses of these classes of configurations reveal that sub-column configurations can be systematically enumerated from regular-column configurations (Shenvi et al., 2013). Meanwhile, for four-component mixture separations, the best plus-column configuration, though having more columns, could never outperform the best regular-column configuration for any given separation in terms of heat duty (Giridhar and Agrawal, 2010a). Therefore, the complete set of regular-column configurations is considered as the proper and reasonable choice of search space of configurations (Giridhar and Agrawal, 2010a). Finally, a regular-column configuration can be further categorized as either *basic* or *thermally coupled* (TC). A regular-column configuration is called basic if each column has one reboiler and one condenser (Agrawal, 2003). A basic configuration does not have thermal coupling but provides the base configuration to synthesize TC configurations. TC configurations can be derived from each basic configuration by replacing one or more of its intermediate heat exchangers with two-way vapor-liquid transfers known as thermal couplings. Introducing thermal couplings to basic configurations rapidly increases the regular-column configuration search space.

These distillation configurations, while all performing the same separation task, have very distinct capital and operating costs. The capital cost of a distillation configuration depends on the number and sizes of distillation columns, reboilers, condensers, and so on. The operating cost of a configuration comprises two major aspects: the total reboiler vapor duty requirement, which is the sum of vapor flows generated at all reboilers per unit time, as well as the temperature level at which the vapor is generated and/or condensed (Agrawal and Fidkowski, 1998a). The first aspect is associated with the first-law heat-duty demand of a distillation configuration, whereas the second is closely related to the heating and cooling utility costs (second-law temperature-level costs) for all reboilers and condensers. One must consider both aspects to accurately evaluate the operating cost of a configuration. Furthermore, due to their structural differences, some configurations are easier to operate and control than others. These concerns naturally raise the following question: "Given a multicomponent separation problem, which distillation configuration(s) is/are more attractive to build, operate, and/or retrofit?"

Identifying attractive distillation configurations for a given separation task requires complete enumeration of all possible configurations in the defined regular-column configuration search space. In an early approach, Thompson and King (1972) provided a method to generate all sharp split configurations. Sargent and Gaminibandara (1976) proposed a superstructure framework to include both sharp and non-sharp split configurations, but this framework was later found to be incomplete. Agrawal (1996) introduced a new class of column arrangements (configurations) that were missing from the superstructure of Sargent and Gaminibandara (1976). Prior to this introduction, in a multicomponent distillation, columns were always arranged sequentially starting from the main feed column. However, in the new "satellite" arrangements of columns, the main feed column communicates with all other columns which are arranged around the central column as its satellites. Still, the problem of enumerating both sharp and non-sharp split n-component regular-column configurations remained unsolved until Agrawal (2003) proposed a rule-based enumeration approach, which laid the foundation for subsequent formulations proposed by Caballero and Grossmann (2004), Ivakpour and Kasiri (2009) and Shah and Agrawal (2010). In particular, Shah and Agrawal (2010) successfully generated the complete search space of all sharp and non-sharp split regular-column configurations using a simple and elegant six-step method, which we refer to as the SA method from hereon.

Once the complete search space for regular-column configurations is generated by the SA method (Shah and Agrawal, 2010), we can apply a series of design strategies to reduce the capital and operating costs of distillation configurations. These strategies and methodologies all fall under the umbrella of process intensification (PI), a concept that has been in use for quite some time but has truly emerged as an important design philosophy in chemical engineering only in the past decade (Segovia-Hernández and Bonilla-Petriciolet, 2016). The idea of PI was first introduced to the chemical industry in the 1970s and has led to some of the brilliant equipment and process innovations that are still being used to this day, such as the static mixer and reactive distillation process (Reay et al., 2013). Over the past decades, PI has attracted increasingly more academic and industrial interest as a guideline for process improvements in designing new facilities as well as retrofitting existing ones to meet the increasing demands for sustainable production. However, the question remains: What really is process intensification? In the 1st International Conference on Process Intensification for the Chemical Industry in 1995, Ramshaw (1995) offered one of the first definitions of PI as a strategy to reduce the size of a chemical plant by reducing the number of unit operations and equipment pieces involved. However, as Stankiewicz and Moulijn (2000) pointed out, Ramshaw's definition is somewhat limited, as it exclusively concerns the reduction of plant and/or equipment size (Ramshaw, 1995). In turn, they broadened the span of PI by redefining it as the development of new equipment and processes that significantly decrease equipment and plant size, reduce waste production, and finally result in cheaper and more sustainable production (Stankiewicz and Moulijn, 2000). Ponce-Ortega et al. (2012) and Reay et al. (2013) further expanded the definition of PI to include principles such as process safety, increase in energy efficiency and production throughput, as well as reduction of inventory and the use of raw materials. Van Gerven and Stankiewicz (2009) envisioned that the future scope of PI would move towards the molecular scale. All these definitions provide valuable insights in understanding what PI means for different industrial applications and scales. In the context of multicomponent distillation, we believe that PI stands for "innovative process synthesis strategies that minimize the number of equipment pieces, reduce total cost, while boosting energy efficiency of multicomponent distillation systems." Under this definition, the overall goal for PI is to synthesize compact, easy-to-operate, energy efficient and cost effective distillation configurations based on a given separation task (Jiang et al., 2018b).

In this review article, we do not aim to extensively discuss the distillation literature but to introduce a comprehensive, multi-layer analysis approach for PI in multicomponent distillation which is summarized in Fig. 1 and discuss the associated relevant literature. Starting from any basic regular-

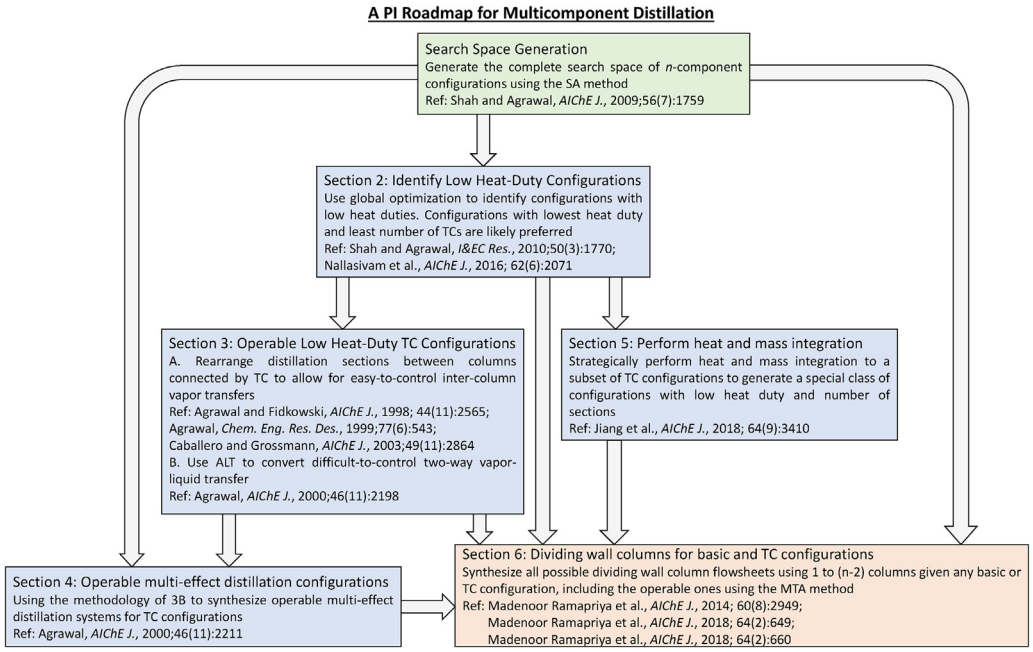

Fig. 1 – A roadmap of PI for zeotropic multicomponent distillation listing the key references that highlight each PI strategy.

column configuration, we first discuss the attractiveness of replacing some or all of intermediate reboilers and/or condensers with thermal couplings in terms of energy and cost savings. This idea is carried over throughout different layers of PI and is the essence of PI in multicomponent distillation. Next, we discuss strategies to reduce or even eliminate the operational difficulties associated with conventional TC configurations, while still retaining their energy and cost benefits. These strategies are highly useful in arriving at the subsequent layers of PI. By applying these strategies, we can synthesize operable multi-effect distillation systems for multicomponent separation to significantly reduce the heat duty requirement. Meanwhile, we can also perform novel simultaneous heat and mass integration in a strategic manner for a selected subset of regular-column configurations. This leads to the discovery of a special class of intensified sub-column configurations that, for many applications, could have the lowest possible total vapor duty requirement among all configurations in the entire search space. Finally, for the first time, we are able to synthesize an array of hitherto unknown dividing wall columns, many of which are operable, for any basic and TC configuration. Through illustrative examples, we provide a comprehensive review of the important layers of PI in multicomponent distillation so that the readers will gain a better understanding as well as appreciation of the great opportunities for PI in multicomponent distillation.

2. Energy-efficient configurations synthesized by introducing thermal couplings

Thermal couplings are two-way liquid–vapor transfer stream between distillation columns within a configuration. Some historical examples of TC configurations include the use of a side-rectifier to recover argon in air distillation (Agrawal and Yee, 1994), and side-strippers to produce different fractions in petroleum crude distillation (Bagajewicz and Ji, 2001). A sequence of TC configurations can be derived from one basic configuration by replacing some or all reboilers and/or condensers associated with intermediate transfer streams, also known as submixtures, with thermal couplings (Petlyuk et al., 1965; Wright, 1949). While some examples of TC configurations have been known for a while, it was not until the 1980s when TC configurations started to receive more attention due to their potential for large heat duty savings (Fidkowski and Krolikowski, 1986, 1987; Agrawal and Fidkowski, 1999; Fidkowski and Agrawal, 2001; Carlberg and Westerberg, 1989). At the same time, the lower heat demand for a TC configuration also leads to smaller diameters for a number of column sections and overall heat exchanger sizes. Together with the elimination of reboilers and/or condensers, introducing thermal couplings strategically can result in lower capital investment and more compact plant being built.

Fig. 2 shows the systematic introduction of thermal couplings to one of the 203 basic configurations synthesized by the SA method (Shah and Agrawal, 2010) for a 5-component *ABCDE* mixture to produce five product streams, each enriched in one of the components. The configuration of Fig. 2a is a basic configuration with no thermal coupling. Instead, it involves one-way liquid transfers of submixtures *BCD*, *CD*, and *DE* as well as one-way vapor transfers of submixtures *ABCD*. In this figure, and also in all subsequent figures, *A*, *B*, *C*, and so on represent pure components with their volatilities decreasing in alphabetical order. Here, *ABCD* could be any industrially relevant mixture such as benzene/toluene/*p*-xylene/*o*-xylene, 1-pentene/pentane/1-hexane/hexane, or water/mono-ethylene glycol (EG)/di-EG/tri-EG, etc. Further, we indicate reboilers by open circles and condensers by filled circles. Starting from the basic configuration of Fig. 2a, submixtures associated with heat exchangers can be systemically replaced by thermal couplings between distillation columns as shown in Fig. 2b–o. Configurations of Fig. 2b–e have one thermal coupling; configurations of Fig. 2f–k have two thermal couplings; configurations of Fig. 2l–o have three thermal couplings; and finally, the configuration of Fig. 2p is completely thermally coupled (CTC), i.e., all submixture heat exchangers within the configuration are replaced by thermal couplings. Overall, for this particular basic configuration of Fig. 2a, there are four submixtures, and there is a possibility to either use or not use TC at each submixture. Therefore, we can derive a total of $2^4 - 1 = 15$ TC configurations, including one CTC configura-

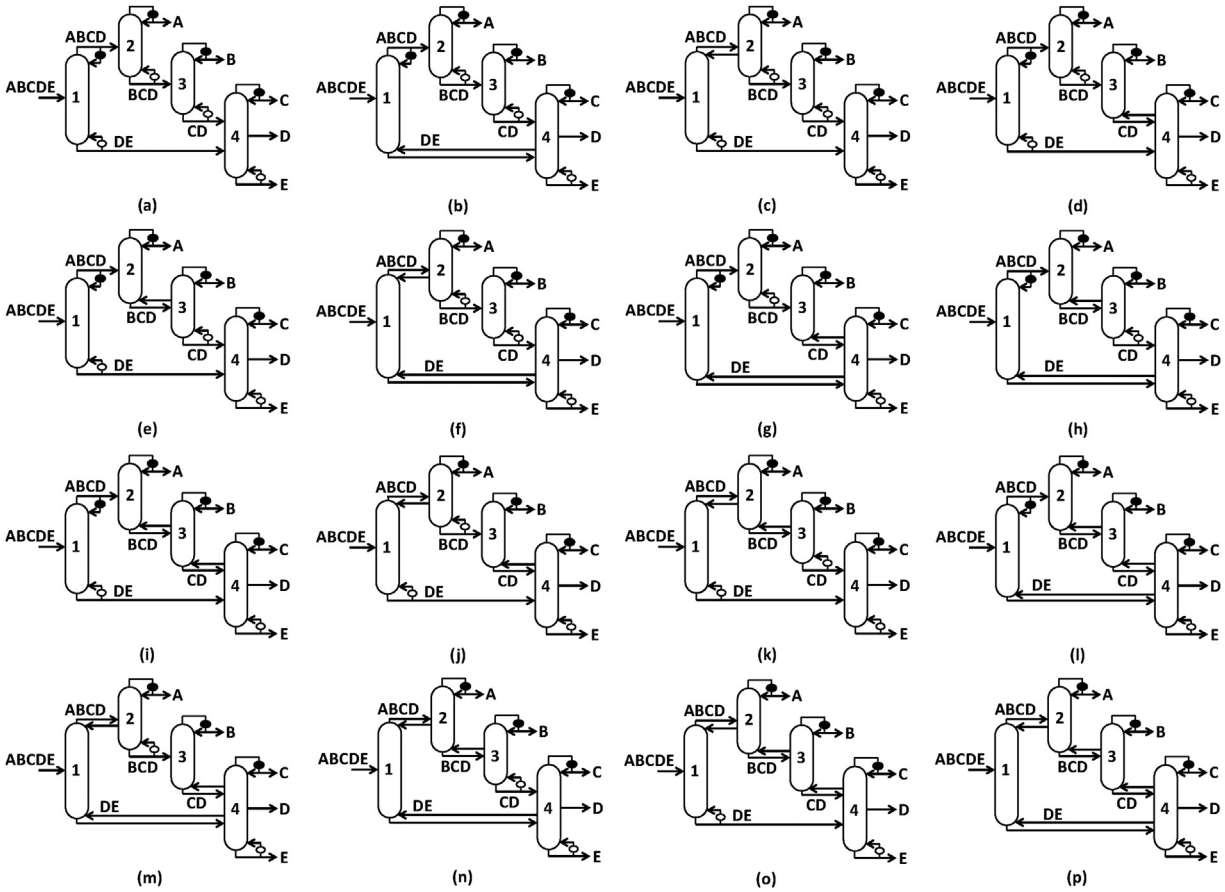

Fig. 2 – A family of regular-column configurations: (a) basic configuration with no thermal coupling; (b–e) configurations with one thermal coupling; (f–k) configurations with two thermal couplings; (l–o) configurations with three thermal couplings; and (p) CTC configuration with all four thermal couplings.

tion and 14 partially TC ones. These configurations have the same column and split arrangement as the basic configuration. The only difference among these configurations is the placement of thermal couplings and heat exchangers at all submixtures. Thus, they can be considered as configurations within the same "family." Each family has a "family tree." In this case, we can draw the family tree for a family of configurations by considering each individual configuration as the parent or child of other configurations. A child configuration contains all the thermal couplings that the parent configuration has, plus one additional thermal coupling. As expected, each family must always have exactly one basic configuration as a starting configuration to generate TC configurations as well as one CTC configuration with complete set of thermal couplings. Also, the configuration of Fig. 2l, even though it has three thermal couplings, is not the child of the configuration of Fig. 2f that has two thermal couplings, including one at submixture *ABCD* which is not present in Fig. 2l.

As the number of components in the feed increases, the number of regular-column configurations increases combinatorially, much faster than that of basic configurations (Shah and Agrawal, 2010). This greatly expands the regular-column configurations search space. Table 1 summarizes the enumeration results of basic and TC regular-column configurations for up to eight-component mixture separations. For instance, for a five-component feed, there exist 203 structurally distinct basic configurations and 5925 TC ones. For six-component feed, the total number of basic configurations is 4373, but the number of TC configurations explodes to 502,539. The large search space of regular-column configurations certainly poses a challenge in identifying the desired configurations for a given separation problem. As a result, there is definitely a need for a quick and reliable screening tool that can accurately evaluate every configuration in the search space within a reasonable amount of computational time (Nallasivam et al., 2013).

To evaluate these configurations, we first need an objective function that characterizes the performance of each configuration quantitatively. The operating cost of a distillation configuration relative to others is often characterized by its total vapor duty requirement, which is the sum of vapor flow generated at all reboilers per unit time at its operating condition. The minimum total reboiler vapor duty requirement, V_{tot}^{min}, is thus a direct representation of a configuration's first-law energy consumption, i.e., heat duty without considering the temperature level at which the heat is produced or rejected (Carlberg and Westerberg, 1989). Therefore, V_{tot}^{min} is commonly used as the objective function for comparing the heat duty requirement of distillation configurations (Nallasivam et al., 2013, 2016).

Due to the combinatorial explosion in the size of regular-column configuration search space with the number of components in the feed (Giridhar and Agrawal, 2010b), evaluating every configuration in the search space rigorously using process simulators such as Aspen Plus is never an easy or efficient option, not to mention the effort required to guarantee convergence and global optimality for each and every simulation flowsheet. One almost always needs to formulate an optimization problem to consider and solve all configurations in the search space in a timely and accurate manner. Caballero and Grossmann (2001) presented a superstructure based on

Table 1 – Complete search space of regular-column configurations synthesized by the SA method (Shah and Agrawal, 2010). The total number of sharp split configurations can be obtained using the closed form formula presented by Thompson and King (1972).

Number of components	Total number of basic configurations	Number of sharp split basic configurations	Total number of TC configurations	Number of sharp split TC configurations
3	3	2	5	2
4	18	5	134	15
5	203	14	5925	98
6	4373	42	502,539	630
7	185,421	132	85,030,771	4092
8	15,767,207	429	29,006,926,681	27,027

state task network representation to synthesize all TC configurations, including the CTC ones. The superstructure was modeled as a generalized disjunctive program. Afterwards, Caballero and Grossmann (2004) extended the superstructure to capture all basic and TC regular-column configurations. The resulting generalized disjunctive program was formulated and solved as a mixed integer nonlinear program (MINLP) to identify the configuration that minimizes the total cost. However, the MINLP could not be solved to global optimality as the local nonlinear programming (NLP) solver failed to give a feasible solution due to convergence difficulties such as singularity issues associated with disappearing column sections (Caballero and Grossmann, 2001). To account for these issues, they proposed an algorithm based on a modified version of logic-based outer-approximation algorithm. Nevertheless, they were still unable to guarantee global optimality with this approach (Caballero and Grossmann, 2001).

Caballero and Grossmann (2004) then introduced a two-step iterative optimization procedure to solve the MINLP by first identifying the best CTC configuration, followed by determining the best submixture reboiler and/or condenser placement for the configuration identified in the first step. They also extended this solution procedure to consider heat integration (Caballero and Grossmann, 2006), column section rearrangements (Caballero and Grossmann, 2003), and dividing wall columns (Caballero and Grossmann, 2013) in their designs. Despite the attempts to solve individual MINLP in each step to global optimality, overall this two-step optimization procedure does not guarantee to always yield the true optimal solution.

Besides the MINLP based approach summarized above, a fundamentally different approach to identify optimal distillation configuration is to first synthesize the complete search space, followed by formulating an individual optimization problem for each configuration in the search space. Inspired by this, Nallasivam et al. (2016) proposed a nonlinear programming (NLP) based approach to determine V_{tot}^{min} for any configuration using Underwood's method for minimum vapor duty calculations in each column section (Underwood, 1949). Jiang and Agrawal (2019) further extended the NLP based approach by Nallasivam et al. (2016) to minimize the total cost for any configuration. It is shown that NLP optimization solvers such as BARON (Tawarmalani and Sahinidis, 2005) guarantee global optimality for each configuration (Nallasivam et al., 2013, 2016). Though this shortcut based algorithm uses underlying assumptions of ideal liquid–vapor equilibrium, constant relative volatility, and constant molar overflow (Nallasivam et al., 2016), it is found that the rank-list of configurations obtained by these NLP calculations is consistent with that obtained by running rigorous Aspen Plus

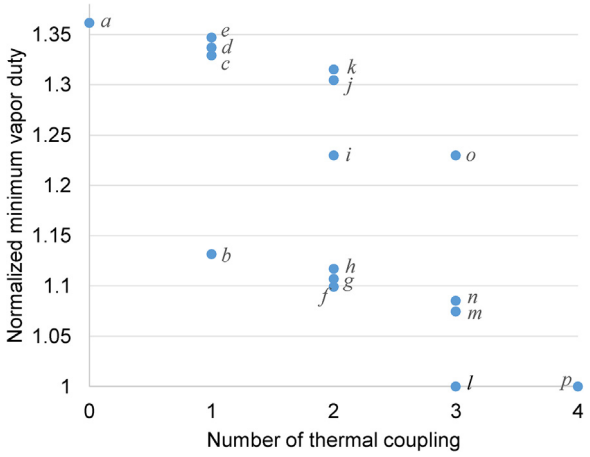

Fig. 3 – Normalized minimum vapor duty requirement of the family of configurations in Fig. 2 with respect to the number of thermal couplings involved. This example deals with feed composition of *abcDE* and relative volatility of $\{\alpha_{AB}, \alpha_{BC}, \alpha_{CD}, \alpha_{DE} = 1.1, 2.5, 1.1, 1.1\}$.

simulations using real thermodynamic models for zeotropic quaternary separations (Madenoor Ramapriya et al., 2018a). This provides the confidence in using the shortcut based method to prune the large search space of configurations shown in Table 1 to a subset of small and manageable number of attractive configurations using the shortcut based method. The attractive subset can then be evaluated in detail using a rigorous process simulator such as Aspen Plus for energy, cost, and other features such as manufacturability and operability.

We evaluated the minimum total vapor duty requirement for the family of configurations considered in Fig. 2. For five-component separations, $2^5 - 1 = 31$ different representative feed compositions can be formulated, depending on whether each component is rich or lean in the feed (Giridhar and Agrawal, 2010a; Jiang et al., 2018a). For example, *ABcDe* denotes that the feed is rich in components *A*, *B*, *D* and lean in components *C* and *E*. Lean components, if there are any, are assigned a mole fraction of 0.05 in the feed, whereas the rich components share the leftover mole fraction equally. Here, we consider the example feed condition of saturated liquid feed with feed composition of *abcDE* (i.e., mole fractions of $A = B = C = 0.05$, $D = E = 0.425$) and flow rate of 1 kmol/s. The relative volatility set considered between each consecutive component is $\{\alpha_{AB}, \alpha_{BC}, \alpha_{CD}, \alpha_{DE}\} = \{1.1, 2.5, 1.1, 1.1\}$, in which an α value of 1.1 is a representative of difficult split and an α value of 2.5 an easy split. The results are summarized in Fig. 3, in which the vertical axis is the normalized V_{tot}^{min} relative to the lowest vapor duty requirement among all configurations

within the family. Data points *a* through *p* in Fig. 3 correspond to the configurations of Fig. 2a through p, respectively. Combining the vapor duty results of Fig. 3 with the configurations shown in Fig. 2, we can easily make the following observations that can be generalized to any family of configurations:

1. Any child configuration must always have a lower or at least the same V_{tot}^{min} as that of any of its parent configurations. Thus, V_{tot}^{min} of any child configuration is always upper bounded by the lowest V_{tot}^{min} among all its parent configurations. For example, as illustrated in Fig. 3, the child configuration of Fig. 2j, which consists of two thermal couplings at submixtures *ABCD* and *CD*, has a lower V_{tot}^{min} than its parent configuration of either Fig. 2c or d.
2. The basic configuration (e.g., point *a* of Fig. 3) and the CTC configuration (point *p* of Fig. 3) must always respectively have the highest and lowest V_{tot}^{min} among all configurations within a family. In this example, the basic configuration requires 36.2% more minimum vapor duty than the CTC configuration.
3. While it is true that introducing thermal couplings to a configuration will never worsen its minimum total vapor duty, it is generally not needed to replace all submixture heat exchangers with thermal couplings (i.e., CTC) to achieve the maximum vapor duty savings (Shah and Agrawal, 2011). In this example, the configuration of Fig. 2l has the same V_{tot}^{min} as the CTC configuration but uses only three thermal couplings. On a similar note, the parent configuration of Fig. 2i, which has two thermal couplings, consumes exactly the same V_{tot}^{min} as one of its child configurations of Fig. 2o.
4. This guideline is concerned with a more fundamental question related to thermal coupling: Is it always more energy efficient to introduce more thermal couplings to a distillation configuration? To answer this question, it is no longer sufficient to focus merely on the absolute value of the total vapor duty requirement irrespective of the temperature levels at which various heat duties are provided and/or rejected (i.e., *first-law heat-duty*) within a configuration. Instead, one also needs to consider the temperature levels at which the vapor duties are produced and condensed, which directly affect the costs of utilities that drive the distillations. This aspect of temperature-level penalty is especially important for sub-ambient temperature distillations, heat pump assisted distillations, as well as applications in which the boiling points of the components involved are very different. For cases of Fig. 2i vs. 2o as well as 2l vs. 2p, it is not useful to include the additional thermal coupling at submixture *ABCD*, since the total vapor duty will not improve any further, and yet the utility cost is likely to increase when the required condensing duty from the condenser at *ABCD* is transferred to the condenser at A which is operated at the lowest temperature level. So, additional thermal couplings no longer provide any additional vapor duty benefits. These extra thermal couplings should be avoided as they could incur unnecessary penalties in utility costs and thus lower the thermodynamic efficiency of the configuration (Carlberg and Westerberg, 1989; Agrawal and Fidkowski, 1998a).
5. On the other hand, in some cases, introducing thermal couplings to certain submixture locations of the configuration would potentially provide significant first-law heat duty savings without bringing any penalties in utility costs. Shah and Agrawal (2011) presented some heuristics to enable quick identification of such useful thermal couplings. For example, we find that when thermal coupling is introduced to the basic configuration at submixture *DE*, the resulting TC configuration of Fig. 2b not only requires the least V_{tot}^{min} of all single TC configurations (Fig. 3), but also requires significantly less minimum vapor duty than configurations of Fig. 2i, j, and k that use two thermal couplings, as well as the configuration of Fig. 2o which uses three thermal couplings. In fact, when closely examining configurations of Fig. 2b, f, and l, which respectively correspond to the "best" TC configurations with exactly one, two, and three thermal couplings from Fig. 3, we recognize that all of them have a thermal coupling at submixture *DE*. To understand this, notice that in column 4, due to the given feed composition, the lower $DE \rightarrow D/E$ split requires significantly more vapor flow than the upper $CD \rightarrow C/D$ split, as the mass flow of component *C* into the column is small compared to that of component *D* or *E*. Therefore, by replacing the reboiler at submixture *DE* with a thermal coupling, the excess vapor duty generated by the reboiler at *E* can now transfer to column 1 to facilitate the $ABCDE \rightarrow ABCD/DE$ split there. As a result, the total vapor duty requirement of the TC configuration of Fig. 2b is greatly reduced compared to that of the basic configuration. At the same time, no additional utility cost due to any increase in vapor duty at a higher temperature level is created. When building energy efficient distillation systems, it is always important to keep in mind the synergistic effect of strategically introducing thermal couplings to the right submixtures in order to achieve the best trade-off between maximum vapor duty savings and low utility costs.
6. So far, we have been analyzing configurations within one family. Now, let us back up from scrutinizing each individual configuration within a family and compare configurations of different families. To do so, we need a common benchmark configuration for comparison. The well-known fully thermally coupled (FTC) configuration is a special CTC configuration that uses the maximum possible number of $n(n-1)$ distillation column sections with $(n+1)(n-2)/2$ submixture transfer streams and only one reboiler and one condenser (Petlyuk et al., 1965; Agrawal, 1996). As an example, the FTC configuration for five-component separation is shown in Fig. 4. It uses a total of 20 column sections, 9 submixture transfer streams, and 6 thermal couplings to replace submixture reboilers and condensers. For ternary and quaternary separations, the FTC configuration always preserves the lowest possible V_{tot}^{min} among all basic and TC configurations in the regular-column configuration search space (Fidkowski and Krolikowski, 1987; Fidkowski and Agrawal, 2001; Halvorsen and Skogestad, 2003; Fidkowski, 2006). For example, for ternary mixture separations, several studies have shown that the FTC configuration can potentially reduce the total vapor duty by 10–50% compared to conventional direct and indirect split basic configurations (Glinos et al., 1986; Triantafyllou and Smith, 1992; Annakou and Mizsey, 1996). For separations involving a higher number of components, it is conjectured (Fidkowski and Agrawal, 2001; Halvorsen and Skogestad, 2003) and later demonstrated (Nallasivam et al., 2016) that the FTC configuration indeed has the maximum total vapor duty benefits compared to any other configuration in the search space. Because of this, for a long time, people believed that the FTC configuration is also more thermodynamically efficient than other configurations for most separations (Triantafyllou and Smith, 1992).

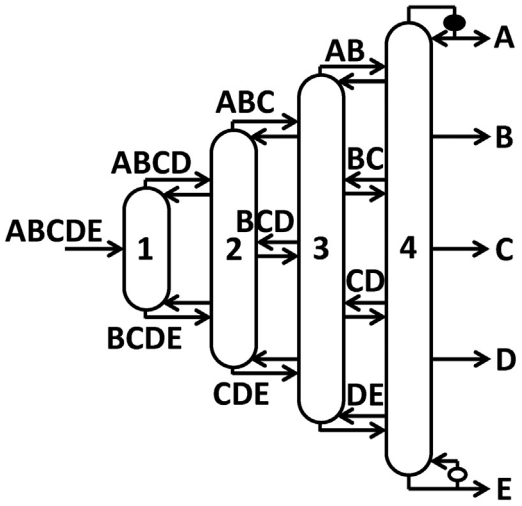

Fig. 4 – Fully thermally coupled (FTC) configuration for five-component mixture separation. Intermediate sidedraws *BCD*, *BC*, and *CD* are two-phase streams that allow both liquid and vapor transfers between distillation column.

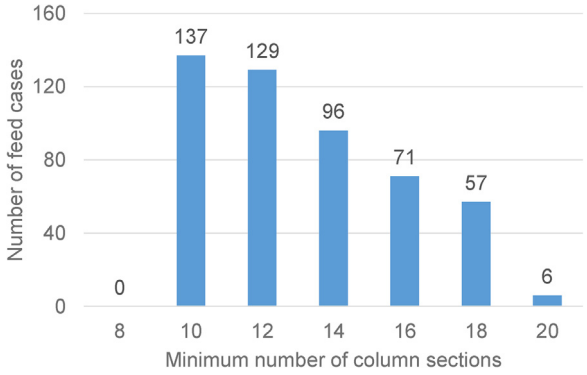

Fig. 5 – The horizontal axis shows the minimum number of column sections required for the configurations to achieve the same V_{tot}^{min} as the FTC configuration. The vertical axis shows the corresponding number of feed cases. Note that for five-component separation, sharp split configurations use $2(n-1)=8$ column sections, whereas the FTC configuration uses $n(n-1)=20$ sections.

However, this contradicts the reality that the FTC configuration has not found wide industrial use (Agrawal and Fidkowski, 1998a), especially for quaternary separations and above. There are many reasons why the FTC configuration is never implemented in large scale, despite being known for nearly 70 years (Wright, 1949). One important reason is that the FTC configuration has the maximum possible number of column sections and submixture transfer streams, which makes it particularly expensive to build and difficult to operate (Abdul Mutalib and Smith, 1998; Wolff and Skogestad, 1995). Nevertheless, another important reason that hinders the FTC configuration from being widely built is that, even though it requires the lowest possible first-law heat duty, this heat is generated at the highest temperature reboiler (e.g., reboiler at *E* of Fig. 4) and rejected at the lowest temperature condenser (e.g., condenser at *A* of Fig. 4). Thus, the actual thermodynamic efficiency of the FTC configuration often turns out to be significantly lower than other configurations in the search space. For ternary separation, Agrawal and Fidkowski (1998a) derived general thermodynamic efficiency equations and conducted detailed analysis to find that the range of feed specifications (composition and relative volatilities) in which the FTC configuration has a higher thermodynamic efficiency than other configurations is quite limited. Flores et al. (2003) also reached similar conclusions when considering a set of cases involving ternary and quaternary separations.

7. Because of observations 3, 4, and 6, one may naturally start questioning: "Does the FTC configuration ever need to be built?" To answer, we need to compare the FTC configuration with other configuration families. Recall the five-component separation example that we previously considered. In this case, for the given feed, it turns out that the partially TC configuration of Fig. 2l, which requires the same minimum total vapor duty as the CTC configuration of Fig. 2p, also achieves identical minimum total vapor duty as the FTC configuration of Fig. 4. Since it uses additional condensers that operate at intermediate temperature levels, the configuration of Fig. 2l preserves the same vapor duty benefits of the FTC configuration while having higher thermodynamic efficiency. Furthermore, this configuration uses only three thermal couplings and ten column sections, half of what is needed for the FTC configuration. Therefore, there is no need to build the FTC configuration for this specific separation task.

   To determine if the above claim is true in general, we generated a total of 496 distinct representative five-component feed specifications following Giridhar and Agrawal (2010a). These feed specifications were synthesized by enumerating all possible combinations of representative feed composition and relative volatility sets (31 representative compositions × 16 representative relative volatilities due to each of the four relative volatilities being either high (2.5) or low (1.1)). We performed exhaustive NLP calculations (Nallasivam et al., 2016) for all 496 feed cases on all 6128 configurations in the search space. From the optimization results summarized in Fig. 5, we found that for almost all the given feed conditions, it is almost always possible to find at least one non-FTC configuration which requires the same V_{tot}^{min} as the FTC configuration while requiring a smaller number of column sections. The FTC configuration uniquely has the lowest V_{tot}^{min} among all configurations in the search space under only 6 out of 496 feed cases (1.2%). And in 137 out of 496 cases (27.6%), the same lowest V_{tot}^{min} can be obtained from configurations with just ten column sections, as opposed to the FTC configuration which requires 20 sections. Furthermore, these non-FTC configurations identified in Fig. 5 have at least one reboiler or condenser that uses milder temperature-level utility, making them more thermodynamically efficient than the FTC configuration. Hence, for most industrial applications, we believe that, unless absolutely needed, building the FTC configuration is never the first choice; that is, it is always possible to find non-FTC substituents that require the same minimum vapor duty as the FTC configuration, yet outperform the FTC configuration in terms of capital investment, compactness, as well as thermodynamic efficiency.

8. Finally, we realize that in our five-component study, none of the sharp split configurations has the same minimum total vapor duty as the FTC configuration in any of the 496 feed cases. This result is consistent with our previous observations for four-component mixture separations that non-sharp split configurations generally have much lower heat duty than sharp split ones (Giridhar and

Agrawal, 2010a). This observation elucidates the importance of including non-sharp split configurations in the search space for finding efficient and low-cost configuration options.

3. Design strategies that improve operability of thermally coupled columns

As mentioned, the operational difficulty associated with thermal couplings is one of the major reasons that impede the construction of FTC or CTC configurations for industrial uses. This is perceived to be due to the opposite directions of vapor transfer streams in two thermal couplings between two distillation columns (Agrawal and Fidkowski, 1998b). Consider, for example, the first two columns of the five-component FTC configuration shown in Fig. 4. The vapor stream associated with the thermal coupling at *BCDE* has to be transferred back from column 2 to column 1, whereas the vapor stream associated with the thermal coupling at *ABCD* is transferred from column 1 to column 2. This means neither column 1 nor 2 could have a uniformly lower or higher pressure than the other column. The pressure profiles within both columns need to be carefully controlled to ensure that the pressure at the bottom of column 1 is always lower than the pressure at the bottom of column 2; and at the same time the pressure at the top of column 1 is always greater than the pressure at the feed point of *ABCD* near the top of column 2. Similar controllability issues are present for subsequent columns as well. As the number of components to be separated increases, the resulting conventional FTC configuration will suffer from increasingly more difficult control and stringent operational requirements, making it less attractive or even impossible for industrial implementation.

The operability issue associated with thermal couplings is not just limited to the FTC configuration. For any TC configuration that has two distillation columns simultaneously connected by two thermal couplings, the vapor flow direction of the top thermal coupling will always be in the opposite direction to that of the bottom thermal coupling. Unless we can find a way to solve the operational challenge, industrial practitioners will be reluctant to build any TC configuration. Here, we discuss two strategies to overcome this operational difficulty from a conceptual design perspective. The first strategy is due to the observation by Agrawal and Fidkowski (1998b), whereby certain configurations with an attractive rearrangement of thermally coupled column sections between the distillation columns provided operable TC configurations (Kaibel, 1987; Smith and Linnhoff, 1988). Some well-known examples include the side-rectifier and side-stripper arrangement derived from the direct and indirect split configuration, respectively (Glinos and Malone, 1985; Liebmann and Dhole, 1995). Agrawal (1999) introduced the concept of thermodynamically equivalent TC configurations, where for any thermal coupling originating from the top/bottom of one distillation column, one can first disjoint the upper/lower column section of the next column from its original location, followed by restacking it right above/below the column from which the thermal coupling originates. Through column section rearrangements, the newly generated configurations are completely thermodynamically equivalent to the original TC configuration, since all we do is to simply reconnect some of the column sections without changing the temperature profile, composition profile, and the *L*/*V* ratio for every column section.

Two examples of thermodynamically equivalent configurations for the five-component FTC configuration of Fig. 4 are reproduced in Fig. 6 from Agrawal (1999). In Fig. 6a, which corresponds to Fig. 6n of Agrawal (1999), the bottommost column sections from columns 2, 3, and 4 have been rearranged to column 1 under thermal coupling at *BCDE*. We find that all thermal couplings, in terms of vapor and liquid splits between different distillation column sections, are identical between the two versions, which provide us with thermodynamically equivalent five-component FTC configurations. In Fig. 6a, column 1 operates at a slightly higher pressure compared to the other three columns to allow for easy transfer of each of the vapor streams. For the same reason, column 2 is at slightly higher pressure than column 3, which in turn is at slightly higher pressure than column 4. If for a given feed separation, it turns out that vapor stream *BCD* needs to be transferred from column 3 to 2, then one could move the top column section from column 3 to the top of column 2 to synthesize yet another thermodynamically equivalent configuration with column 3 being operated at higher pressure than column 2, as shown in Fig. 6b. Clearly, several thermodynamically equivalent configurations can be generated for any given FTC configuration. Agrawal (1999) provided the following observations to ensure operability between TC columns: (i) The reboiler associated with the heaviest component and the condenser associated with the lightest component are in different columns; (ii) The distillation column associated with reboiler is operated at a slightly higher pressure than other columns; (iii) The distillation column associated with a condenser is operated at a slightly lower pressure compared to other columns; (iv) The column associated with the heaviest component reboiler does not receive, but only provides, vapor streams to other columns, and (v) The column associated with the lightest component condenser does not provide and only receives vapor streams from other columns. Caballero and Grossmann (2003) applied the concept of thermodynamically equivalent TC configuration to generate the complete set of thermodynamically equivalent configurations for any given TC configuration.

As examples of thermodynamically equivalent configurations, consider the TC configuration shown in Fig. 7a. This configuration has four thermal couplings at submixtures *ABCD*, *CDE*, *AB*, and *DE*. As a result, a total of $2^4-1=15$ thermodynamically equivalent versions can be systematically derived. In Fig. 7b–e, we show 4 out of these 15 thermodynamically equivalent versions that involve only one column section rearrangement. It can be easily verified that, in the original configuration of Fig. 7a, the vapor transfer streams of thermal couplings at submixtures *ABCD* and *CDE* flow in opposite directions, making it hard to control. Among the four thermodynamically equivalent versions shown in Fig. 7, those of Fig. 7c and e overcome the operational difficulty as both vapor streams associated with thermal couplings *ABCD* and *CDE* are now transferred unidirectionally from one column to the other. By simply maintaining the column from which the vapor streams are supplied at a slightly higher pressure than the other column, the flow of both vapor transfers can be easily regulated through a valve. At the same time, the liquid streams can be transferred through static head or liquid pumps (Agrawal and Fidkowski, 1999).

Besides resolving the operational difficulty from a conceptual design perspective, there are two additional apparent advantages of performing column section rearrangement to

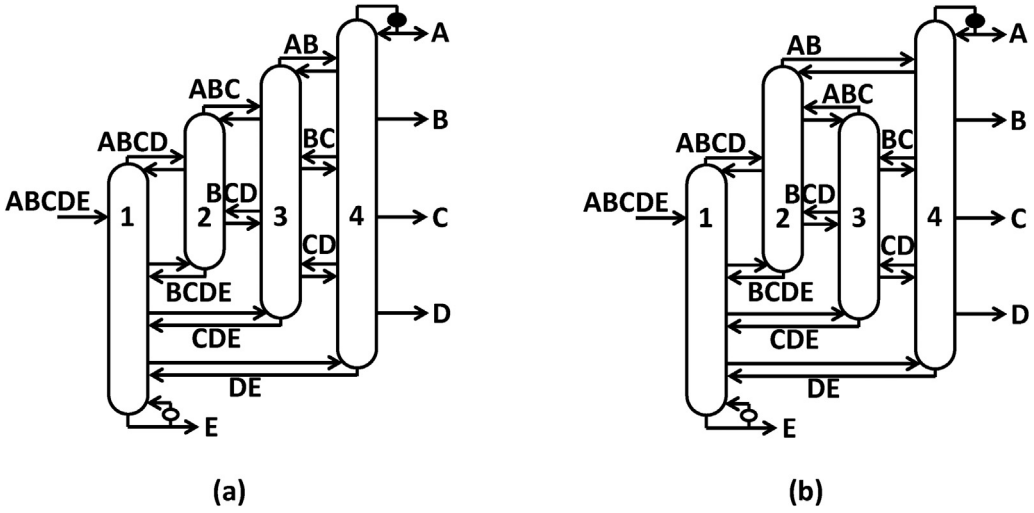

Fig. 6 – Two possible thermodynamically equivalent configurations for the five-component FTC configuration reproduced from Agrawal (1999). (a) and (b) correspond to Fig. 6n and o in Agrawal (1999), respectively.

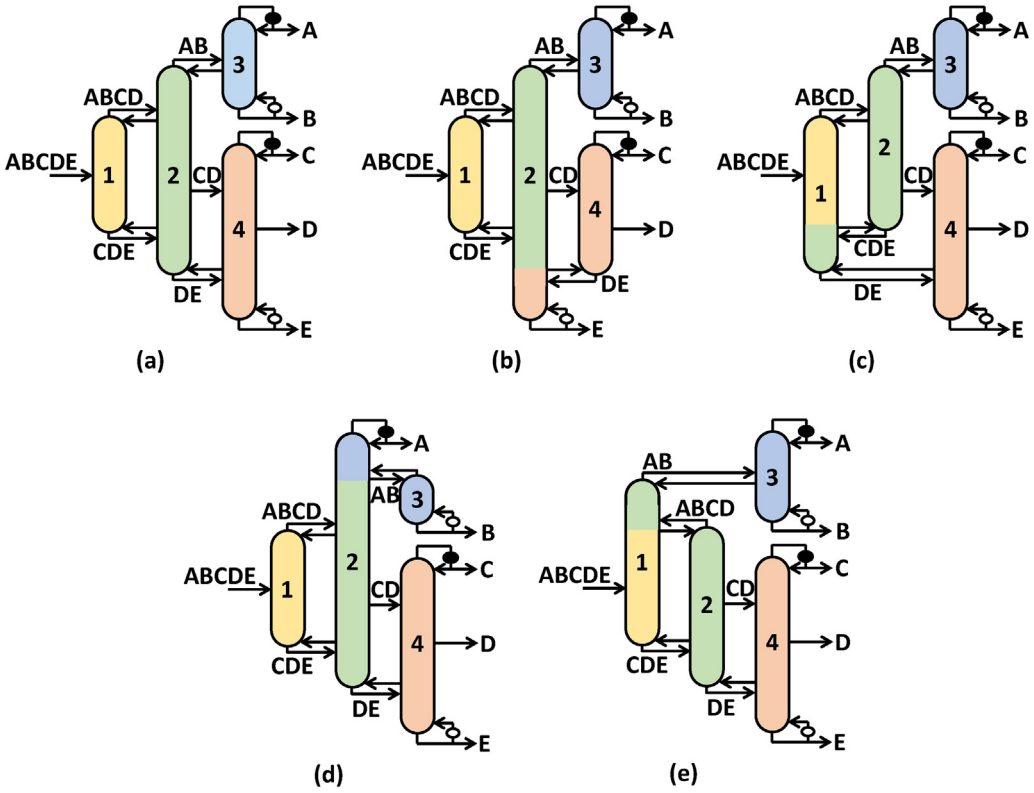

Fig. 7 – (a) A five-component CTC configuration; (b–e) thermodynamically equivalent versions of (a) by rearranging one column section. There are 11 more thermodynamically equivalent versions that can be further derived by rearranging more than one section simultaneously. Note that the sidedraw stream *CD* is withdrawn from the column 2 as saturated liquid.

TC configurations. The first advantage, as we have discussed, is due to the thermodynamic equivalence nature of these newly derived arrangements compared to the original TC configuration. Therefore, as long as we start from a TC configuration that has been identified to be energy efficient, the new equivalent versions are guaranteed to be energy efficient as well. To some extent, this strategy allows us to gain operational ease "for free" without sacrificing any heat duty benefits. The second advantage is that, through column section rearrangement, some equivalent versions may have lower capital costs compared to the original configuration if sections with similar vapor duty (i.e., similar diameter) are now stacked together. Hence, column section rearrangement might be a useful technique for any TC configurations, even those with no operational difficulties associated with the opposite direction of vapor flows. Again, consider the configuration of Fig. 2f and the same case study discussed in the previous section. In this configuration, since the two thermal couplings of column 1 connect to two different columns (column 2 and column 4), column 4 can then be operated at slightly higher pressure than column 1, which is itself maintained at slightly higher pressure than column 2. No operational difficulty related to vapor transfers will be experienced. However, since most of the vapor duty generated at column 4 reboiler is transferred through thermal coupling at *DE* to column 1, the diameter of the original column 4 is likely to shrink above the location

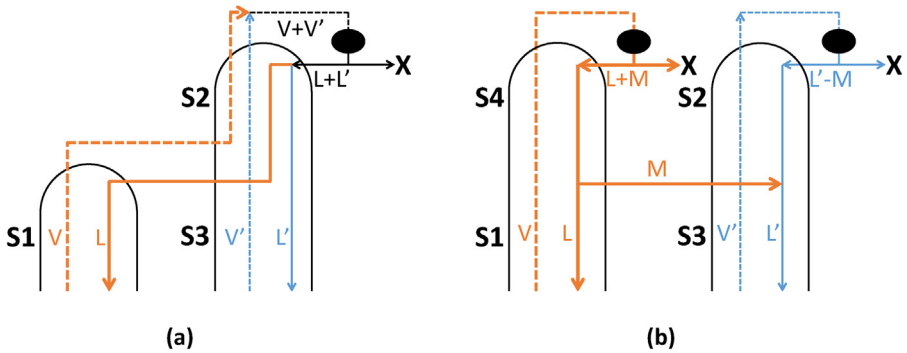

Fig. 8 – (a) A conventional TC arrangement that produces product or submixture stream X; (b) TC arrangement of (a) replaced with ALT stream M and a new section S4 on top of S1. Note that the orange (thicker) lines indicate liquid and vapor flows that belong to the first column, whereas the blue (thinner) lines indicate liquid and vapor flows that belong to the second column. Dashed lines represent vapor flow paths and solid lines represent liquid flow paths.

where the *DE* stream is introduced, resulting in higher capital cost. By restacking the bottom section of column 4 below column 1, the resulting new arrangement is expected to be cheaper to build, as the column sections are better rearranged so that the newly stacked columns have more uniform diameters.

Based on the discussion so far, one might conclude that the root cause of the operational challenge associated with thermal coupling comes from the vapor transfer, which is inherently more difficult to control than a liquid transfer stream. A bold but reasonable question one can then ask is: "Is there a way to keep the energy benefit of a thermal coupling while getting rid of vapor transfer completely?" Agrawal (2000b) provided a solution by introducing a method for converting any conventional thermal coupling, originally as a two-way liquid–vapor transfer, into only liquid transfer stream as the second strategy for improving operability. Fig. 8 illustrates Agrawal's liquid transfer (ALT) conversion for a two-way thermal coupling which originates at the top of a column. The procedure is quite simple and yet powerful. First, duplicate the upper part of the column (including any associated product or stream) associated with net material inflow and stack the duplicated part onto the column associated with net material outflow. After that, change the two-way liquid–vapor thermal coupling link to an ALT stream. For example, in the configuration of Fig. 8b, a new section S4, which is a duplication of section S2 along with its associated condenser and final product *X*, is placed on top of section S1. The thermal coupling that connects the two columns is then converted into an ALT stream with liquid flowrate of *M*. Based on physical reasoning, Agrawal (2000b) concluded that the new configuration of Fig. 8b will have the same overall vapor duty requirement as the original TC configuration of Fig. 8a, and hence, is thermodynamically equivalent to the original configuration.

Madenoor Ramapriya et al. (2014) presented a mathematical proof by showing that a physically feasible flowrate *M* in Fig. 8b for the ALT stream must always exist such that the *L*/*V* ratio of section S4 $\left(\frac{L+M}{V}\right)$ and section S2 $\left(\frac{L'-M}{V'}\right)$ in the new configuration is identical. And it is also equal to the *L*/*V* ratio of section S2 $\left(\frac{L+L'}{V+V'}\right)$ in the original configuration of Fig. 8a. A similar proof can be constructed when a thermal coupling that originates from the bottom of a column is converted to an ALT stream. We can easily visualize the thermodynamic equivalence between the two arrangements of Fig. 8 by tracing their liquid and vapor flow paths. By having a two-way liquid–vapor transfer in the TC configuration of Fig. 8a, the vapor and liquid traffic inside section S1, combined with those in section S3, are transferred respectively to and from section 2 where the single condenser is located. Therefore, when thermal coupling is in place, both the separation tasks that take place in sections S1 and in S3 are assigned to the condenser on top of section S2. However, by adding an additional section S4 on top of S1 and placing a new condenser on top of S4, we simply redirect the vapor and liquid traffic inside section S1 so that, instead of diverting them, respectively, to and from the next column, they now stay inside the same column. By doing so, the new section S4 and the condenser on top of it are used exclusively for the separation inside section S1. This also enables section S2 as well as the condenser on top of it to focus entirely on its own separation task inside S3. The configuration of Fig. 8b requires the same total vapor duty as the original TC configuration by manipulating flowrate *M* of the ALT stream, which can be easily accomplished with a valve. At the same time, the additional condenser on top of S4 also gives extra controllability to the configuration of Fig. 8b. Therefore, this approach successfully solves the operational difficulty associated with vapor transfer in a conventional thermal coupling and allows us to come up with a sequence of operable designs that are thermodynamically equivalent to the conventional TC configuration that we started with.

In Fig. 9, we draw some of the equivalent configurations derived from the configuration of Fig. 7a whereby conventional two-way thermal couplings are replaced with ALTs. Note from Fig. 9 that the operational benefit associated with each conversion of a thermal coupling to one-way ALT comes with a price of an additional column section and a heat exchanger. However, the number of heat exchangers can be reduced by collecting the overhead vapor/bottom liquid streams that produce the same product and sending them to a common condenser/reboiler containing separate passages. Each passage is designed with a tailored active heat transfer area to match the approach temperature required for condensing/vaporizing the associated vapor/liquid stream (Agrawal and Madenoor Ramapriya, 2016). The overall active heat transfer area of the common heat exchanger will be similar to the sum of active heat transfer areas for all individual exchangers, as the overall total vapor duty requirement remains the same. Alternatively, the vapor/liquid streams for common condensers/reboilers can be first combined, condensed/vaporized together, and then redistributed to the columns with valves and pumps. For example, in Fig. 9a, the pressure of the higher pressure vapor stream at *A* can be reduced and mixed with

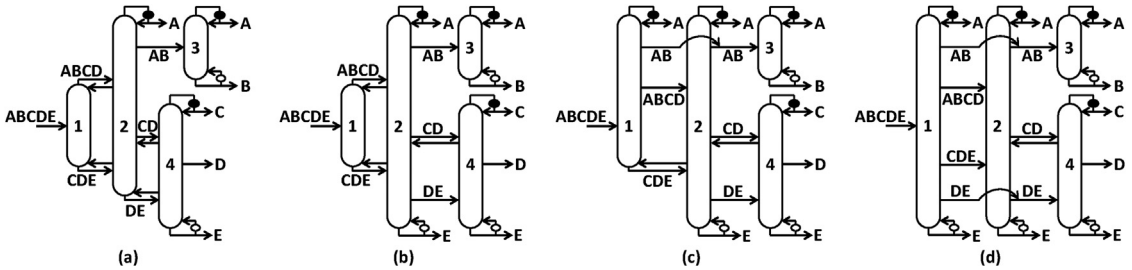

Fig. 9 – Equivalent configurations of Fig. 7a by replacing two-way thermal couplings with ALT stream (a) at submixture *AB*; (b) at submixtures *AB* and *DE*; (c) at submixtures *ABCD*, *AB*, and *DE*; (d) at submixtures *ABCD*, *CDE*, *AB*, and *DE*.

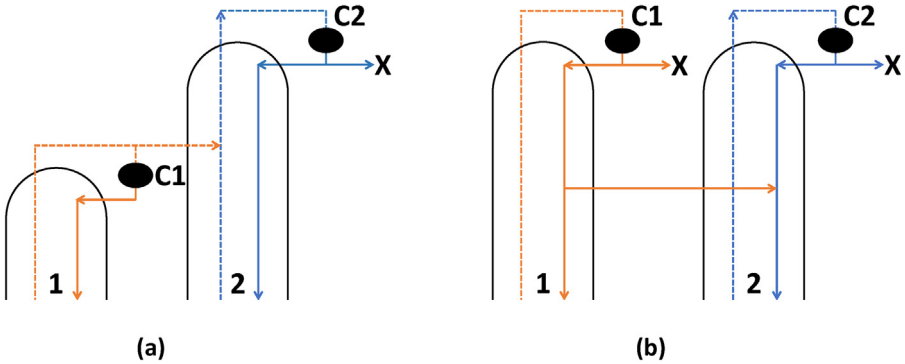

Fig. 10 – (a) The distillate stream of column 1 is associated with condenser C1 and transferred as saturated vapor to column 2 where the final pure product *X* is produced by condenser C2; (b) the ALT arrangement of TC column of Fig. 8a. Both condensers produce final pure product *X*.

the other *A* stream, the combined stream is condensed and a fraction of liquid is pumped to the top of the higher pressure column as reflux. Similarly, in Fig. 9b, the lower pressure liquid at *E* is increased in pressure either using static head or a pump and then mixed with higher pressure liquid *E*; the combined stream is vaporized and a fraction of the vapor is provided to the lower pressure column across a valve for boilup.

Agrawal's liquid transfer method (Agrawal, 2000b), apart from offering operability convenience, provides additional benefits: (i) reduction in heat duty due to thermal coupling becomes clear; (ii) double-effect and multi-effect distillations for TC columns, in order to further reduce heat duty, become feasible; and (iii) new dividing wall column configurations including those which are more operable can be drawn.

To understand (i), first consider the conventional arrangement of Fig. 10a where the submixture stream produced as the top product of column 1 is associated with a condenser C1. This submixture is fed to column 2 as saturated vapor stream. And the liquid reflux of column 1 is generated by condensing part of its overhead vapor in C1. In column 2, final pure product *X* is produced by condensing all the vapor coming from the vapor feed as well as the vapor flow below the feed point in the column. In contrast, as we can see from the ALT arrangement of Fig. 10b that is thermodynamically equivalent to having a thermal coupling at the submixture, the condenser C1 of column 1 has moved up as a new column section is added and now participates in distilling a portion of the pure product stream *X*, i.e., sharing part of this separation task originally belonging to C2 as shown in Fig. 10a. Furthermore, condenser C1 in the ALT arrangement also provides the liquid reflux required for column 1. This suggests that, the demand for condensing duty of C2 of Fig. 10b is less than that of Fig. 10a. If the split associated with the top of column 2 is critical and controls the overall vapor duty requirement in the column, then this leads to an overall reduction in heat duty of the entire ALT arrangement of Fig. 10b (i.e., the TC configuration) compared to the basic configuration of Fig. 10a. In this case, placing the condenser C1 at submixture location in Fig. 10a lowers the separation efficiency in terms of heat duty by unnecessarily condensing part of the overhead vapor as a submixture and losing the opportunity to use the same condensing duty to perform further distillation in column 1. Such inefficiency in the basic configuration of Fig. 10a is generally manifested in the literature through the discussion of so-called "remixing losses" caused by thermodynamic irreversibility when a single-phase submixture stream enters column 1 as reflux (Amminudin et al., 2001; Hernández et al., 2003).

Up till this stage, we have been discussing the advantages of building TC configurations over basic configurations as well as addressing the operational issues associated with conventional thermal couplings through innovative PI strategies. These approaches and insights related to thermal couplings, when combined with other existing PI strategies such as multi-effect distillation, simultaneous heat and mass integration, and dividing wall columns, can create an amazing array of synergistic possibilities that produces numerous attractive distillation configurations hitherto unknown to us. The remaining discussions will be devoted to describing these combinations.

4. Energy efficient, operable multi-effect distillation for thermally coupled configurations

One of the first and direct applications of all PI strategies discussed earlier is the synthesis of energy efficient and operable multi-effect distillation systems for TC configurations. Multi-effect distillation, which involves distillation columns operating at different pressures, performs various heat integrations between the condenser associated with a

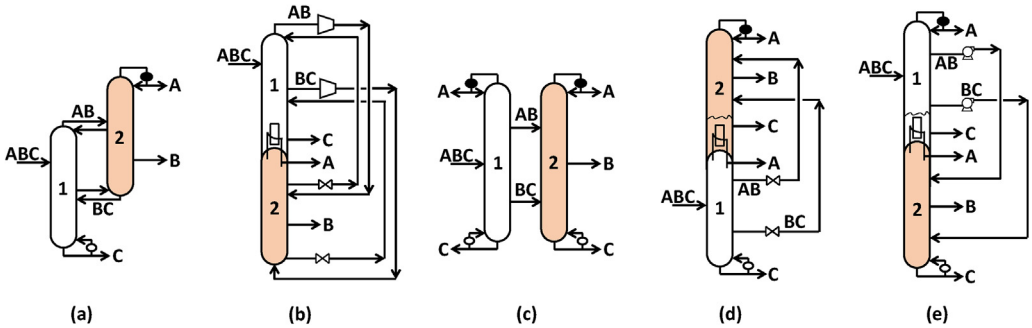

Fig. 11 – (a) Ternary FTC configuration; (b) initial attempt to draw a double-effect configuration from (a); (c) equivalent configuration of (a) by converting all thermal couplings to ALT streams; (d) operable double-effect configuration using forward heat integration (adapted from Agrawal (2000a)); (e) operable double-effect configuration using reverse heat integration.

higher-pressure column and reboiler at a lower-pressure column. Through heat integration, the overall heat usage of the distillation system can be significantly reduced. Wankat (1993) performed detailed calculations for a series of double- and multi-effect distillation configurations for binary mixtures and concluded that these configurations could lead to significant heat duty savings with only a modest increase in capital cost. For ternary separations, Cheng and Luyben (1985) found that double-effect configurations derived from conventional basic direct-split, indirect-split, and prefractionator schemes could result in 20–45% decrease of heat duty requirement. Although the overall savings of heat duty depends on the feed composition and relative volatilities as well as the operating conditions for both columns, double-effect distillation has the potential to reduce heat duty up to 50% over basic configurations (Agrawal, 2000a; Engelien and Skogestad, 2005). Several control studies also showed that these double-effect versions of basic configurations could be quite operable (Ding and Luyben, 1990; Mizsey et al., 1998).

Moreover, a number of parametric analyses for ternary distillations (Annakou and Mizsey, 1996; Emtir et al., 2001; Rév et al., 2001) demonstrate that double-effect systems for basic configurations outperform the best TC configuration in almost all feed conditions. These results are striking given that TC configurations already consume significant less heat duty than the basic configurations. It makes a process designer naturally wonder if it is possible to introduce multi-effect distillation to TC configurations to achieve even greater heat duty savings.

Following the conventional procedure to draw the double-effect version from a basic configuration, an initial attempt (Agrawal, 2000a) to draw a double-effect configuration is shown in Fig. 11b for the ternary FTC configuration of Fig. 11a, which is an operable thermodynamically equivalent version of the Petlyuk column (Petlyuk et al., 1965) and can be easily synthesized by using column section rearrangement described earlier (Agrawal, 1999). The main feature of the configuration of Fig. 11a is that the reboiler and condenser are associated with different columns, thereby allowing their linking through double-effect heat integration. In the double-effect configuration of Fig. 11b, the vapor streams of thermal couplings *AB* and *BC* are first compressed and then sent to the high-pressure column 2, whereas the liquid streams of both thermal couplings are transferred from the high-pressure column 2 to low-pressure column 1. There is no reboiler or condenser in this configuration to generate vapor or liquid externally, which introduces a difficult challenge for column startup. Specifically, since the high-pressure column 2 has no external source for vapor generation, all the vapor duty required for column 2 must be supplied by the vapor streams from the low-pressure column 1 via thermally couplings. But at the same time, the vapor duty for column 1 is in turn generated by the heat obtained from condensing the vapor from the top of the column 2. This endless-loop type scenario makes the startup and operation of such a double-effect configuration especially challenging. To build multi-effect configurations for TC separations that are operable, it would be desirable to include external heating and cooling utilities for distillation instead of relying solely on the vapor and liquid flows transferred via thermal couplings.

Agrawal (2000a) introduced a method using ALT as the right tool to solve this operability issue, and his method will now be illustrated through Fig. 11. Fig. 11c with ALTs is one of the equivalent configurations of the FTC configuration of Fig. 11a. It has a reboiler and a condenser in each column, making it similar to a basic configuration such as a prefractionator from a process control perspective. From this equivalent configuration, we can then draw the corresponding double-effect system in which the overhead vapor of one column is heat integrated with bottoms liquid of the other column. This double-effect configuration will be fully operable. Two possible operable double-effect configurations, one with forward heat integration (feed enters the high-pressure column) and the other with reverse heat integration (feed enters the low-pressure column), are shown in Fig. 11d and e. In comparison with the initial drawing of the double-effect configuration in Fig. 11b, these new configurations produce pure products *A* and *C* from both columns. Each column has either a condenser or a reboiler, making the startup and operation of the double-effect configuration much easier.

As another example, we examine some of the possible double- and multi-effect arrangements for the configuration of Fig. 9d, which we recall is an equivalent configuration of Figs. 9a and 7a. With a total of four columns, many operable double-effect arrangements are possible. For instance, any two of these four distillation columns can be heat integrated through double-effect. The other two columns can either be double-effect heat integrated or left without such heat integration. For each combination of these columns, there are again two possible schemes: forward heat integration or reverse heat integration. Alternatively, any three of the four columns or all the four columns can be multi-effect heat integrated by creating/operating the distillation columns at three or four different pressures, respectively. All these arrangements are operable.

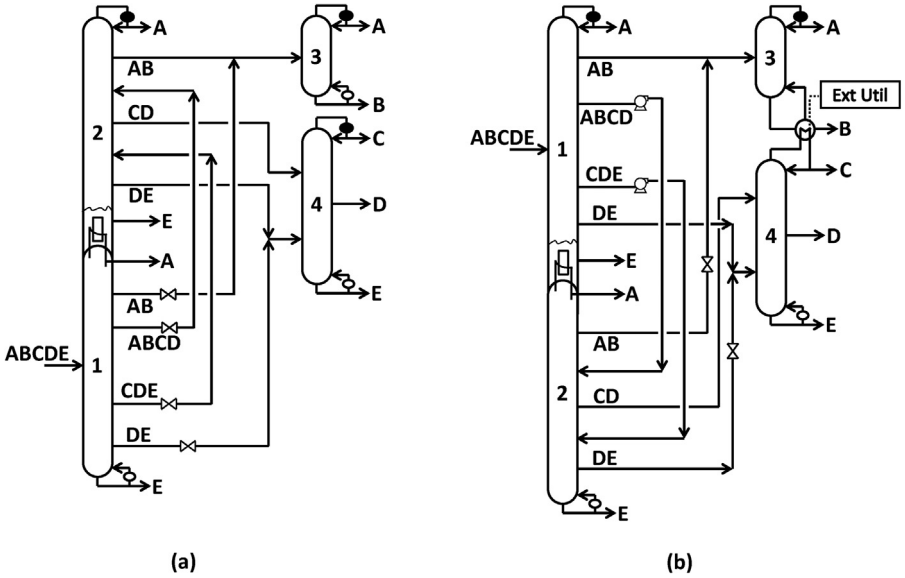

Fig. 12 – (a) Operable double-effect configuration with forward heat integration between column 1 and column 2 for the configuration of Fig. 11d; (b) operable double-effect configuration with reverse heat integration between column 1 and column 2, with column 3 and column 4 being heat integrated at the same pressure (external heating or cooling utilities may be needed). Note that columns 3 and 4 in (b) can be operated at the same pressure as column 1.

Fig. 12 shows two possible double-effect configuration designs. In the first configuration of Fig. 12a, double-effect forward heat integration takes place between the top of the column 1 and bottom of column 2. Columns 3 and 4 can be operated at any suitable pressure. In the second configuration of Fig. 12b, we present a double-effect configuration with reverse heat integration between the top of column 2 and the feed column. In this configuration, columns 3 and 4 are heat integrated without creating any pressure difference, since the pure product *B* produced at the bottom of column 3 is lighter than the pure product *C* produced at the top of column 4. As a result, there is a sufficient temperature gradient allowing for heat integration between column 3 and column 4, which reduces the overall heat duty and increases energy efficiency even further. We will discuss this specific type of distillation configuration in detail in the context of simultaneous heat and mass integration in the next section.

Per our earlier discussion, one generally will not need all four thermal couplings shown in Fig. 7a to achieve the maximum heat duty benefit. For a given feed to be separated, it is very likely that most, if not all, of the heat duty benefit can be achieved with one or two thermal couplings. This means that the number of ALT streams between columns 1 and 2, in an optimized version of the configuration of Fig. 12a or b, will be substantially lower than those currently shown in Fig. 12 and will contribute towards the attractiveness of the configuration. In conclusion, the PI strategy of converting thermal coupling to ALT stream opens up a window of new operable multi-effect distillation opportunities for TC configurations.

A word of caution towards finding the lowest heat-duty multi-effect configuration with low heat duty: once the lowest heat duty subset of regular-column configurations with or without thermal couplings has been identified through global optimization, it is not guaranteed that their multi-effect versions will yield the lowest heat-duty multi-effect options. Reduction in heat duty, when two columns are integrated through a double effect, depends on how close the heat duties are for each of the columns prior to and after the integration. When the two columns have nearly equal heat duty requirements, a potential reduction of 50% could be realized. Thus, one can envision a scenario where a configuration has an overall higher heat duty, but due to better matching between the heat duties of the columns, leads to lowest heat duty subsequent to multi-effect integration. This calls for an independent optimization of the multi-effect configurations.

5. Attractive thermally coupled configurations synthesized by novel heat and mass integration strategy

Heat and mass integration (HMI) to consolidate distillation columns in a configuration is mostly known as simultaneous elimination of a reboiler and a condenser, producing the same final product streams or submixtures. HMI of this kind has been commonly used to synthesize regular-column configurations (Shenvi et al., 2013; Giridhar and Agrawal, 2010a; Ivakpour and Kasiri, 2009; Sargent and Gaminibandara, 1976; Agrawal, 1996; Caballero and Grossmann, 2001; Rong et al., 2003). However, HMI is not just limited to removing reboilers and condensers associated with the same final products or intermediate streams. For example, in the 4-component basic sharp split configuration shown in Fig. 13a, the bottom product *B* produced at column 2 is lighter than the top product *C* produced at column 3. Therefore, instead of using two independent columns, we can consolidate columns 2 and 3 to form a single column 2–3, as drawn in Fig. 13b, in which the vapor generated at the reboiler of *D* and the liquid produced by the condenser at *A* now, respectively, provide the vapor and liquid flow needed for both $AB \rightarrow A/B$ and $CD \rightarrow C/D$ splits. The resulting configuration, first synthesized by Brugma (1942), can reduce the overall heat duty significantly when compared to the parent configuration of Fig. 13a. Further, with the expense of an additional column section in column 2–3, the Brugma configuration simultaneously reduces the number of distillation column shells by one, a reboiler that originally produces product *B*, and a condenser that originally produces product *C*. Both final product streams *B* and *C* are now withdrawn from column 2–3 as liquid sidedraws. Such

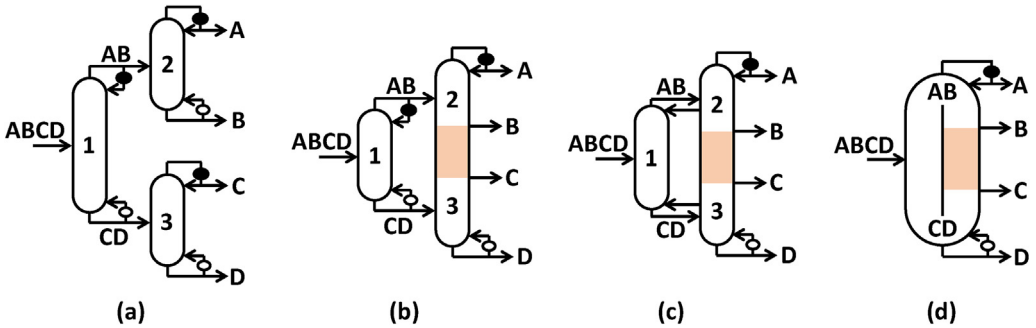

Fig. 13 – (a) A 4-component basic sharp split configuration; (b) the Brugma configuration (Brugma, 1942); (c) the Cahn and Di Miceli configuration (Cahn et al., 1962); (d) the Kaibel column (Kaibel, 1987).

HMI achieved by means of an additional section is referred to as heat and mass integration with additional section, or simply HMA (Madenoor Ramapriya et al., 2015). The additional section is called the HMA-section and is provided with enough stages to allow smooth heat and mass transfer between the ascending vapor from the lower part and descending liquid from the upper part of the column (Shenvi et al., 2013). The resulting capital and operating costs reduction due to HMA makes it attractive for industrial applications.

According to generalization of Brugma's concept (Brugma, 1942) by Madenoor Ramapriya et al. (2015), HMA can be introduced between any two distillation columns so long as the bubble point of the liquid stream leaving the condenser to be eliminated is higher than the dew point of the vapor stream leaving the reboiler to be eliminated, since it guarantees the required approach temperature for heat transfer to happen. It suggests that, in theory, HMA can take place between any two distillation columns if one column produces a less volatile top final product/submixture stream, whereas the other column produces a more volatile bottom final product/submixture stream. Thus, systematic enumeration of all HMA opportunities can generate numerous new HMA configurations (Madenoor Ramapriya et al., 2015). For example, for the basic configuration of Fig. 14a, the reboilers associated with submixture *BC* and/or final product *C* can be heat and mass integrated with condensers associated with submixture *DE* and/or final product *D*. This leads to a total of six possible combinations of HMA arrangements. In addition, for each of the six HMA configurations synthesized, one can further draw its TC derivatives. Two of the thermally coupled HMA configurations are illustrated in Fig. 14b and c. Note that in the configuration of Fig. 14c, when there is liquid and vapor traffic between column sections 2 and 3, such mass flow leads to heat duty penalty as it does not provide some of the distilling duty needed to produce portions of final products *C* and *D*. Therefore, the configuration of Fig. 14c is strictly not thermodynamically equivalent to the configuration of Fig. 14b.

Additional thermodynamically equivalent HMA configurations can also be generated by converting some of the two-way thermal couplings with the ALT streams (Agrawal, 2000b). For instance, consider a new HMA configuration (Jiang et al., 2018a) drawn in Fig. 14e, which is thermodynamically equivalent to the HMA configurations of Fig. 14b. This new HMA configuration is obtained from the CTC version of Fig. 14a by first converting thermal couplings at *BC* and *DE* with ALTs, as shown in Fig. 14d, followed by performing two HMAs between columns 2 and 3 as well as between columns 4 and 5. Notice that final product streams *C* and *D* are now withdrawn from the resulting configuration of Fig. 14e as liquid sidedraws from two different consolidated columns. This technique, also known as strategic side-stream withdrawal, was first discovered by Shenvi et al. (2013) as a new way to further reduce the heat duty of a slightly modified version of Fig. 14c by making streams *BC* and *DE* as liquid sidedraws instead of two-way liquid–vapor transfers. It is now clear that this heat duty reduction is really attributed to the combined effect of thermal coupling and heat integration as illustrated through Fig. 14a and d leading to 14e. This also verifies the observation made by Shenvi et al. (2013) that pure *C* and *D* can be produced as sidedraws in the consolidated column 2–3.

Although HMA can potentially reduce the overall heat duty, it may lead to higher utility costs since the reboiler and condenser operated at intermediate temperature levels are simultaneously eliminated due to HMA. To minimize the utility costs, one can introduce intermediate reboiler/condenser at appropriate locations of the consolidated column (Madenoor Ramapriya et al., 2015; Shenvi et al., 2013). Suppose, for the HMA configuration of Fig. 14e, the upper $ABC \rightarrow A/BC$ split is more energy intensive than the lower $DEF \rightarrow DE/F$ split in column 2–3, while the lower $DE \rightarrow D/E$ split is more energy intensive than the upper $BC \rightarrow B/C$ split in column 4–5. Then, for column 2–3, instead of generating all the required heat for both splits at the reboiler of *F* which operates at the highest possible temperature level, an intermediate reboiler can be placed at sidedraw product *C* to generate the extra heat duty needed for the upper $ABC \rightarrow A/BC$ split. Similarly, for column 4–5, instead of rejecting all the heat at the condenser of *B*, an intermediate condenser can be placed at sidedraw product *D* to condense the excess vapor from the lower $DE \rightarrow D/E$ split. Similarly, if needed, an intermediate reboiler or an intermediate condenser could also be used at either *C* or *D* product location in the configuration of Fig. 14b. The key message is that, starting from a basic configuration, the concept of HMA, especially when combined with other PI strategies, can lead to numerous new and potentially attractive HMA configurations. Among all the new HMA configurations synthesized from the basic configuration of Fig. 14a, the one which always has the lowest overall heat duty requirement and meanwhile has the highest degree of structural simplicity is shown in Fig. 14b. For example, this configuration, which is thermodynamically equivalent to the HMA configuration of Fig. 14e that requires 14 column sections to build, only uses 11 column sections. Such HMA configurations of Fig. 14b share the unique feature of the existence of a thermal coupling at every submixture and HMA only between pure component products. By virtue of this feature, Jiang et al. (2018a) showed that such a configuration minimizes the remixing losses caused by thermodynamic irreversibil-

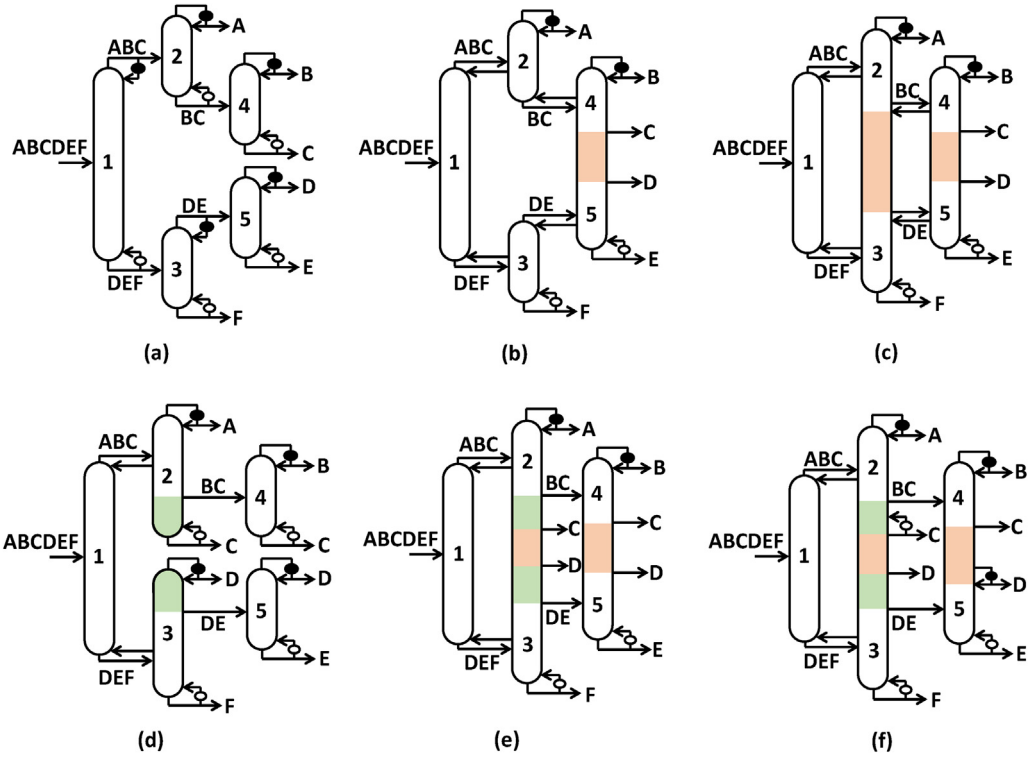

Fig. 14 – (a) A 6-component basic configuration; (b) the HMP configuration derived from (a) by coupling reboiler at *C* with condenser at *D*; (c) another thermally coupled HMA configuration derived by coupling reboilers *BC* and *C* with condensers *DE* and *D*, respectively; (d) thermodynamically equivalent configuration of the CTC version of (a) with ALTs; (e) a HMA configuration derived from (d) containing two HMAs. This configuration is thermodynamically equivalent to the HMP configuration of (b), but has more column sections and sidedraws; (f) the same configuration of (e) with an intermediate reboiler at *C* in column 2–3 and an intermediate condenser at *D* in column 4–5 to reduce the temperature-level penalty when *ABC → A/BC* split requires more heat duty than *DEF → DE/F* split in column 2–3, and *DE → D/E* split requires more heat duty than *BC → B/C* split in column 4–5.

ity among all possible HMA configurations synthesized from a basic configuration. Thus, following the method of Jiang et al. (2018a), for each basic configuration synthesized by the SA method (Shah and Agrawal, 2010), we first quickly check if there simultaneously exists any reboiler that produces a pure component product that is more volatile than any final pure component product produced from a condenser. If so, HMA at submixture level is not required for this configuration to achieve the maximum heat duty savings. Instead, delaying HMA until the final product ends followed by introducing complete thermal coupling to replace all submixture heat exchangers leads to a new, energy efficient HMA configuration which we refer to as the **HMP configuration** whose name highlights the aspect that HMA is only introduced between two final product streams (Jiang et al., 2018a).

Table 2 summarizes the enumeration results of HMP configurations for up to six-component mixture separations (Jiang et al., 2018a). The second and third columns of Table 2 list the total number of basic configurations and the subset of basic configuration identified as HMP candidates, respectively. For a four-component system, there exists one and only one candidate basic configuration shown in Fig. 13a that can undergo HMP. The resulting HMP configuration of Fig. 13c is readily derived from the Brugma configuration by introducing complete thermal coupling to submixture *AB* and *CD*, and is due to Cahn et al. (1962). For five-component system, all 15 basic configurations that are candidates for HMP have been explicitly drawn and can be seen in the paper by Jiang et al. (2018a). Note that some basic configuration candidates can lead to more than one HMP configurations. This multiplicity has been accounted for as listed in the last column of Table 2. The fourth column of Table 2 specifies the number of sharp split basic configuration candidates for HMP. These values are consistent with the results of Rong et al. (2003) who only investigate sharp split HMP configurations. As one can see, with increasing number of components in the feed, the subset of sharp split HMP configurations constitutes a continually shrinking fraction of the set formed by all HMP configurations.

Among all possible HMA arrangements for a basic configuration, the HMP configuration features the principles of PI the most since it exhibits the maximum heat duty savings due to both thermal coupling and HMA and also has the simplest structure to build. Through several case studies of five-component separations, Jiang et al. (2018a) quantify the magnitude of potential heat duty savings for the first time by introducing HMP to basic configuration candidates. They show that many HMP configurations can often even have the same V_{tot}^{min} as the FTC configuration of Fig. 4, which as mentioned before always yields the lowest V_{tot}^{min} among all regular-column configurations in the search space (Fidkowski and Krolikowski, 1987; Fidkowski and Agrawal, 2001; Nallasivam et al., 2016; Fidkowski, 2006). For example, consider the CTC configuration of Fig. 7a from which one of the 17 HMP configurations for five-component separations, as shown in Fig. 15a, can be directly synthesized by consolidating column 3 and column 4. This HMP configuration uses 3 columns, 13 column sections, 5 intercolumn submixture transfers, and 4 thermal couplings, as opposed to having 4 columns, 20 sections, 9 submixture

Table 2 – The number of basic configurations that are candidates for HMP and the number of HMP configurations for up to 6-component separation.

Number of components	Total number of basic configurations	Total number of basic configuration candidates for HMP	Number of sharp split basic configuration candidates for HMP	Total number of possible HMP configurations
4	18	1	1	1
5	203	15	6	17
6	4373	282	26	347

Source: Jiang et al. (2018a).

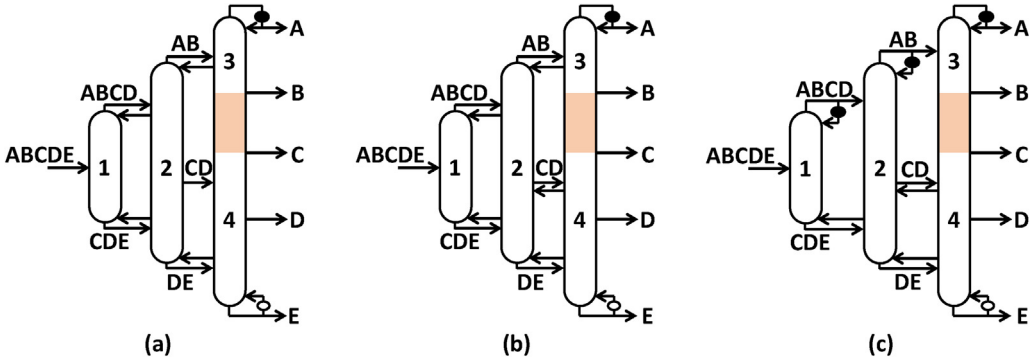

Fig. 15 – (a) HMP configuration derived from the configuration of Fig. 7a. In this configuration, the sidedraw stream *CD* is taken out from column 2 as saturated liquid, as shown in Fig. 7; (b) the same HMP configuration of (a) allowing two-phase flow for sidedraw stream *CD*; (c) a partially TC configuration derived from the configuration of (b) by introducing condensers back to submixtures *ABCD* and *AB*.

transfers, and 6 thermal couplings for the FTC configuration of Fig. 4.

As an illustration of potential benefits, we consider the case in which the relative volatility set between each consecutive component is $\{\alpha_{AB}, \alpha_{BC}, \alpha_{CD}, \alpha_{DE}\} = \{2.5, 2.5, 1.1, 1.1\}$. Extensive NLP calculations for all 31 (i.e., $2^5 - 1$) representative feed compositions, each as saturated liquid, were conducted and the following observations were made. (1) The HMP configuration of Fig. 15a gives exactly the same V_{tot}^{min} as the FTC configuration for 12 cases of the feed compositions. Note that in this HMP configuration, sidedraw stream *CD* is withdrawn from column 2 as a liquid-only stream which is expected to be easier to control than a two-phase stream. However, if we relax this restriction by allowing the sidedraw *CD* to be a two-phase stream (same as for the FTC configuration of Fig. 4), then the number of feed composition cases under which the corresponding HMP configuration of Fig. 15b achieves the same V_{tot}^{min} as the FTC configuration increases from 12 to 19. For the remaining 12 cases, the HMP configuration has a slightly higher V_{tot}^{min} than the FTC configuration, but no more than 3.5%. (2) More interestingly, extensive NLP calculations for all HMP as well as regular-column configurations disclose that, among all the configurations that give the same V_{tot}^{min} as the FTC configuration, the one that requires the fewest number of column sections corresponds to one of the HMP configurations under a number of feed conditions. From a practitioner's perspective, this suggests that the HMP configurations are capable of providing the most heat duty savings and capital cost reductions to a wide window of feed conditions. (3) For some cases, the heat duty saving benefits are preserved even when some thermal couplings in the original HMP configuration are replaced back with heat exchangers (Jiang et al., 2018a). For instance, for the same relative volatility set considered above, when the thermal couplings at submixtures *ABCD* and *AB* are replaced with condensers for the HMP configuration of Fig. 15b, the resulting partially TC configuration, shown in Fig. 15c, still has the same V_{tot}^{min} as the FTC configuration for 16 out of 31 feed composition cases. Note that now every column has at least one reboiler and/or condenser, which makes the configuration of Fig. 15c much more effective to operate than the FTC configuration. These observations also support our earlier argument that, for a given separation task, it is almost always possible to synthesize some non-FTC configurations through various PI strategies that would require the same heat duty savings as the FTC configuration, but are more thermodynamically efficient and cost-effective.

6. Systematic synthesis of all dividing wall columns for any conventional TC distillation configuration

Lastly, we now present how one can combine all the PI strategies together to synthesize all useful dividing wall columns (DWCs) using a single column shell or multiple shells ranging from 2 to $n-2$ for any TC configuration, including any HMP configuration. But first, we briefly discuss the historical evolution of the DWCs. The first DWC due to Wright (1949) to separate a ternary mixture feed into three product streams is shown in Fig. 16b. It is easy to observe that Wright's DWC is thermodynamically equivalent to the ternary FTC configuration of Fig. 16a, also known as the Petlyuk configuration (Petlyuk et al., 1965), and has the same low heat duty as the liquid and vapor flow rates in various column sections remain unchanged. To achieve this, a vertical partition is placed inside the distillation column shell to create two separate zones that allows different separation tasks to take place within the same column without disturbing each other's heat and mass transfer. These two zones essentially mimic the prefractionator (column 1) and the main column (column 2) of the original FTC configuration. The thermal couplings at *AB* and *BC* in the FTC configuration are in turn transformed into a free space that allows for two-way liquid–vapor communication above

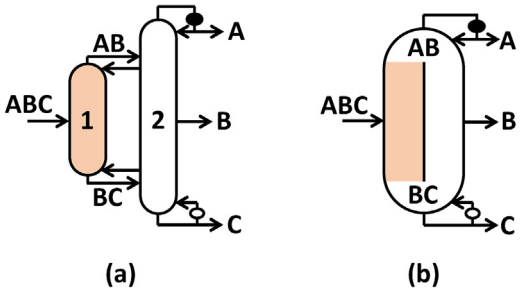

Fig. 16 – (a) The three-component FTC configuration; (b) DWC version of (a) proposed by Wright (1949).

and below the partition, respectively. As a result, the DWC of Fig. 16b is completely thermodynamically equivalent to the original FTC configuration of Fig. 16a. The second known DWC due to Kaibel (1987) to separate a quaternary mixture into four product streams is shown in Fig. 13d. The Kaibel column is identical in performance to the HMP configuration of Cahn and Di Miceli (Cahn et al., 1962) in Fig. 13c and has the same low heat duty as the HMP configuration.

It is clear that neither of the two DWCs intrinsically result in operating cost reduction by themselves. Rather, they do have a potential for considerable amount of capital cost as well as land requirement savings as they reduce the number of column shells and other equipment pieces used for distillation. As much as 30% of capital cost reduction for ternary separations has been reported as DWCs are used in place of conventional sharp split configurations (Lestak and Collins, 1997; Schultz et al., 2002; Kolbe and Wenzel, 2004; Dejanović et al., 2010). Thus, the compactness and cost effectiveness of DWC makes it an exciting path for PI in multicomponent distillation.

In the 1987 paper (Kaibel, 1987), Kaibel also suggested DWC arrangements to separate feed mixtures containing more than four components. These can be classified into two categories. The first one was an extension of the DWC arrangement shown in Fig. 13d. Basically, sharp-split HMP configurations (see Table 2) using one column shell with multiple dividing walls of the kind shown in Fig. 13d were proposed. In the second category, a series of connected DWCs of either the kind shown in Fig. 16b or 13d are used to separate a mixture containing higher number of components. From the discussion in Sections 2 and 5, it is clear that for a given multicomponent separation, none of the two categories guarantee low heat duty or the lowest heat duty. To overcome this challenge, Christiansen et al. (1997) suggested dividing wall column arrangements for the FTC as well as satellite configurations (Agrawal, 1996). Their DWCs for a quaternary mixture are shown in Fig. 17. They introduced an additional dividing wall within the column shell to account for the thermally coupled third column in the configuration. Note that in the FTC configuration DWC of Fig. 17b, the second dividing wall has a hole to allow vapor and liquid traffic associated with submixture *BC* to pass from one side to the other. For Agrawal's satellite column, in addition to the DWC shown in Fig. 17d, Christiansen et al. (1997) also suggested a clever triangular wall structure to allow unimpeded transfer of liquid and vapor streams from the feed side to the satellite columns. Such triangular dividing walls and the associated DWC structures have been described in detail by Agrawal (1999).

A common characteristic of all the DWCs suggested until 1997 is that all the dividing walls start at an intermediate location and terminate at an intermediate column of the column shell. Optimal operation of such DWCs is particularly challenging, as it is difficult to achieve the desired vapor split at the bottom of a dividing wall. For example, consider the DWC of Fig. 16b, the vapor flow generated at the reboiler of *C* cannot be regulated as it travels upwards and gets split by the partition. Therefore, the control of vapor flows in the two parallel zones created by the dividing wall is missing in this DWC. Depending on the liquid split on each side, the vapor flow splits in order to maintain an equal pressure drop on each side of the partition. And it is difficult to operate and maintain the DWC at the optimal *L*/*V* ratio in either parallel zone. As a result, for many feed conditions, the heat duty benefits from the DWC due to thermal couplings may not be realized. In fact, a much higher heat duty is generally required in practice to achieve the desired product purity. This challenge gets compounded for higher-component DWCs such as the ones in Fig. 17, as the number of unregulated vapor splits increases with the number of dividing walls. Because of this, so far we have not seen any industrial implementation of DWC with two or more dividing walls.

As one can see, use of one or more dividing walls within a column shell reduces the number of columns resulting in capital cost reduction. However, for a widespread exploitation of this benefit, it is essential that easy methods to control vapor split across a dividing wall/partition be provided. The first such solution whereby vapor split is controlled by means external to the column shell was provided by Agrawal (2001). For ternary and quaternary mixture separations, Agrawal suggested a number of TC DWCs where a dividing wall is extended to at least one of the ends of the column shell, whereby its vapor flow can now be controlled either at the condenser located at the top end of the column or at the reboiler located at the bottom end of the column. Two ternary TC configuration examples due to Agrawal (2001), one for the side-stripper

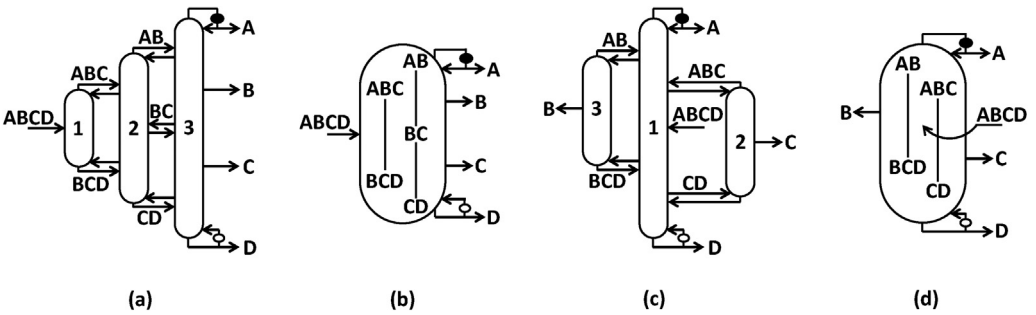

Fig. 17 – DWCs due to Christiansen et al. (1997) for the FTC configuration and Agrawal's satellite column arrangement. (a) The four-component FTC configuration; (b) DWC version of (a); (c) An Agrawal's satellite column arrangement; (d) DWC version of (c).

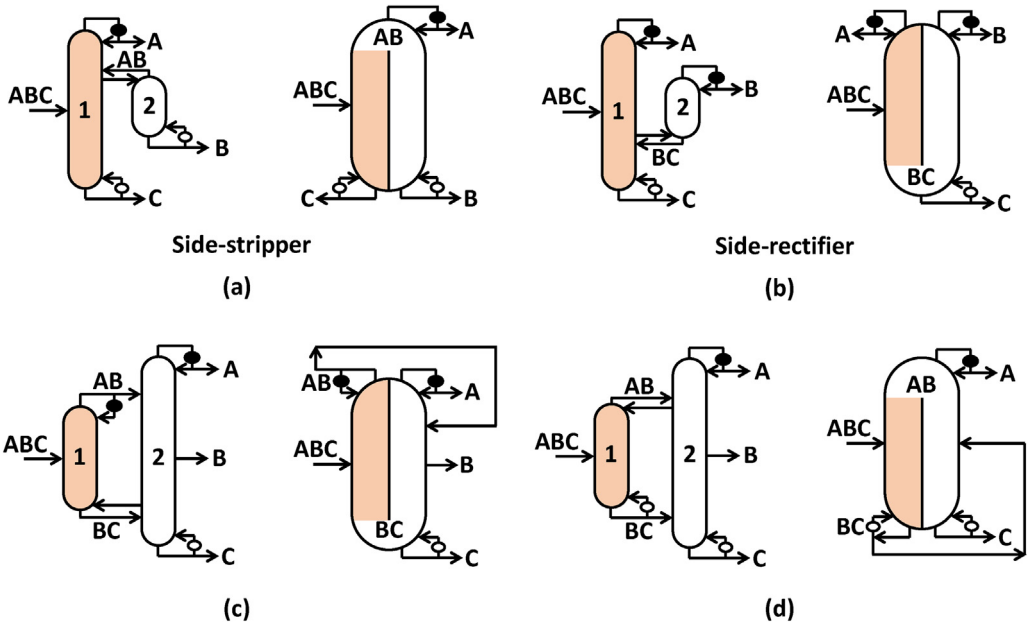

Fig. 18 – (a) Equivalent configuration of ternary FTC configuration of Fig. 16a by using ALT at thermal coupling *BC*; (b) the resulting DWC of (a); (c) equivalent configuration of ternary FTC configuration by using ALT at thermal coupling *AB*; (d) the resulting DWC of (c); (e) the DWC derived from the configuration of Fig. 11c.

and the other for the side-rectifier, are shown in Fig. 18a and b. For the side-stripper case of Fig. 18a, it is clear that the vapor flow on each side of the dividing wall can be easily controlled with reboilers associated with final products *B* and *C*. Similarly, for the side-rectifier case of Fig. 18b, the vapor flow rate on each side can be controlled by either adjusting the ΔT across each of the condenser heat exchangers or through the use of a valve in one of the vapor lines. Also, we point out that in the literature, DWCs by Ognisty and Manley (1998) and Monro (1938) have been incorrectly referred to as side-strippers and side-rectifiers, as their proposed structures do not have proper thermal coupling and thus do not benefit from a lower heat duty associated with thermal coupling (Dejanović et al., 2010; Madenoor Ramapriya et al., 2018c). As discussed in Section 2, for many feed conditions, other CTC configurations provide the same low heat duty as the FTC configuration. Therefore, for such feed conditions, Agrawal's DWCs shown in Fig. 18a and b will have the same lowest heat duty as for the Wright's DWC of Fig. 16b, plus the added benefit of being able to externally control the vapor flow on each side of the partition.

Recently, Agrawal and coworkers have introduced a slew of DWCs along with a systematic method to draw DWC arrangements for any given TC configuration (Agrawal and Madenoor Ramapriya, 2016; Madenoor Ramapriya et al., 2014, 2016, 2018b,c). Before discussing these findings in detail, let us finish the discussion related to TC DWCs for ternary mixture separations. Two more TC DWCs from Madenoor Ramapriya et al. (2018c) are shown in Fig. 18c and d. These TC DWCs have the same feature regarding vapor flow controls on each side of the partition as compared to the DWCs shown in Fig. 18a and b. From Table 1, for a ternary feed mixture, there are a total of five TC configurations – four of these are drawn as DWCs in Fig. 18 and the fifth one, which is the FTC configuration, in Fig. 16b. Again, we emphasize that for most feed conditions, it is possible to find at least one non-FTC TC configuration that also has the same lowest heat duty as the FTC configuration (Agrawal and Fidkowski, 1999). Thus, for most ternary separations, a process designer would be able to choose one of the DWCs from Fig. 18 to provide the lowest heat duty along with the flexibility to control vapor flows externally to the column.

Now, consider a less common feed composition case in which the FTC configuration solely has the lowest heat duty and is the most attractive option to build. One is now faced with the following question: "Is there a way to draw an equivalent DWC for Wright's DWC (i.e., Fig. 16b) that will preserve the heat duty benefits while providing external control of the vapor split across the partition similar to DWCs shown in Fig. 18?" The solution to this question is provided by Agrawal and Madenoor Ramapriya (2016). They applied ALT to the conventional two-way thermal coupling and created equivalent DWCs with one-way liquid transfers. Starting from the original FTC configuration of Fig. 16a containing two thermal couplings, 3 (i.e., $2^2 - 1$) additional equivalent configurations can be synthesized by using ALT at thermal coupling *AB*, or at thermal coupling *BC*, or at both thermal couplings *AB* and *BC*. These equivalent configurations and their resulting DWCs are drawn in Fig. 19. Any of the three equivalent DWCs is now equipped with at least one reboiler and/or condenser for each of the two zones created by the partition, which allows independent precise control of *L*/*V* ratio in each zone. Thus, the DWCs shown in Fig. 19 no longer suffer from the controllability issue that is associated with the conventional DWC of Fig. 16b.

An important feature of each dividing wall created by the technique of Agrawal and Madenoor Ramapriya (2016), which has been absent from all the previously introduced dividing walls in the literature, is the transfer of an intermediate liquid stream from one side of the partition to an intermediate location on the other side of the partition. Transfer of liquid stream *BC* in Fig. 19, liquid stream *AB* in Fig. 19d, as well as both liquid streams *AB* and *BC* as shown in Fig. 19e are such examples. This kind of liquid transfer across a dividing wall can be easily accomplished and Fig. 20 illustrates an example. Descending liquid stream containing *AB* is collected from the feed side of the partition in collection pot 1, transferred to the other side, mixed with the descending liquid there in collec-

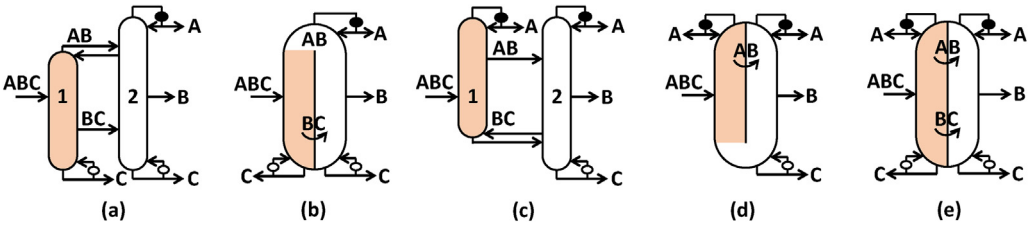

Fig. 19 – (a) Equivalent configuration of ternary FTC configuration of Fig. 16a by using ALT at thermal coupling *BC*; (b) the resulting DWC of (a); (c) equivalent configuration of ternary FTC configuration by using ALT at thermal coupling *AB*; (d) the resulting DWC of (c); (e) the DWC derived from the configuration of Fig. 11c.

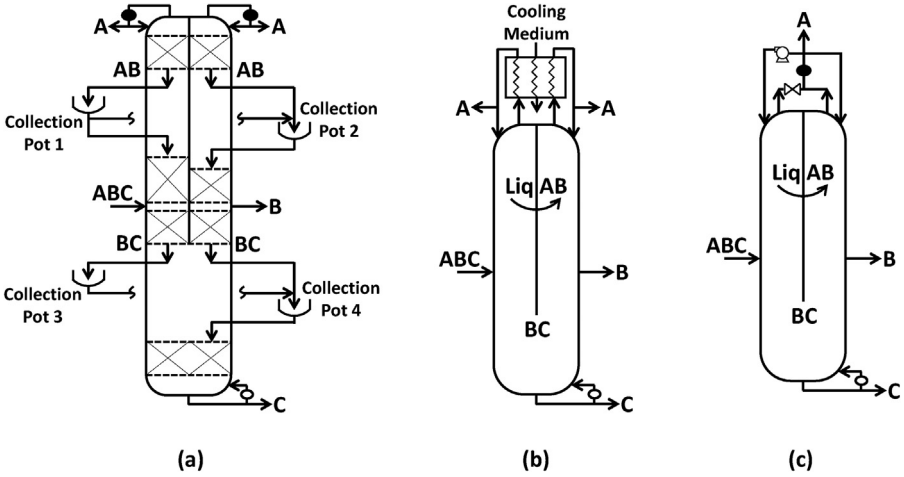

Fig. 20 – Feasible operating options for DWC of Fig. 19d. (a) A method to transfer liquid stream *AB* across the dividing wall; (b) A combined heat exchanger to condense two overhead vapor streams of *A* in separate passages; (c) The two overhead vapor streams of *A* are mixed by reducing the pressure from the higher pressure side of the dividing wall, followed by condensing and then pumping a portion of the liquid stream to the higher pressure side as reflux. Alternatively, pump could be replaced with a static head to feed the liquid.

tion pot 2, and then fed to an intermediate section on the other side of the partition producing final product *B*. There are also various other options to consolidate the two condensers associated with *A* or the two reboilers associated with *C* in Fig. 19. In Fig. 20b and c, we show two alternative options for consolidating the two condensers associated with final product *A*. Similar arrangements can be provided at the reboiler end for final product *C* (Agrawal and Madenoor Ramapriya, 2016).

Any of the DWC shown in Figs. 16b, 18 and 19 for ternary separations can also be used to distill a feed mixture containing more than three components to produce three product streams. Now some of the product streams will not be pure products but a mixture of components present in the feed stream. In such cases, configurations in Fig. 19 may be attractive as they allow the possibility of producing two final product streams of *A* or *C* with different compositions while requiring low heat duty. This observation is also valid for DWCs created for ≥4-component feeds (Madenoor Ramapriya et al., 2014, 2016).

Now we introduce an easy-to-use, step-wise method of Madenoor Ramapriya, Tawarmalani, and Agrawal (MTA). The MTA method is the first available method that can synthesize the complete set of single- and multi-shell DWC for any distillation configuration (Madenoor Ramapriya et al., 2018b,c). Here we consider some of the relevant results from the MTA method and reader is directed to the original papers for details. The MTA method is capable of generating DWCs for basic configurations that have no thermal coupling as well, but here we are focusing on TC configurations, as they lead to lower heat duties. Consider the quaternary FTC configuration of Fig. 17a, which has the lowest heat duty but also challenges associated with vapor split across two dividing walls. The MTA method generates a total of 36 DWCs, including the one of Fig. 17b, all of which are thermodynamically equivalent to each other (Madenoor Ramapriya et al., 2016). Among these 36 DWCs, 15 of them are easy-to-operate DWCs utilizing Agrawal and Madenoor Ramapriya (AMR) dividing walls. As discussed above, the key characteristic of an AMR dividing wall is that, at thermal coupling locations, only liquid streams are transferred across the wall. Fig. 21a shows one of the 15 DWCs that contain two AMR dividing walls. Similarly, an easy-to-operate DWC for the five-component FTC configuration of Fig. 4 is shown in Fig. 21b. It is now clear that it has become feasible to draw easy-to-operate FTC DWCs for any *n*-component mixture separation ($n \geq 3$).

Another important outcome of the MTA method is that for a given *n*-component feed mixture, one can systematically synthesize an array of energy efficient DWC configurations ranging from one column shell up to $n-2$ column shells. This work thus greatly expands the search space of useful configurations for separating a multicomponent mixture. We illustrate this with respect to the five-component HMP configuration discussed earlier in Fig. 15a and b. The original configuration contains three column shells, and the application of the MTA method allows us to generate configurations with one (Fig. 22a to f as examples) and two (Fig. 22g as an example) column shells. In Fig. 22, when the sidedraw stream *CD* is transferred as a liquid stream, then it is equivalent to the HMP configuration of Fig. 15a. On the other hand, when *CD* is transferred as a two-way liquid–vapor communication

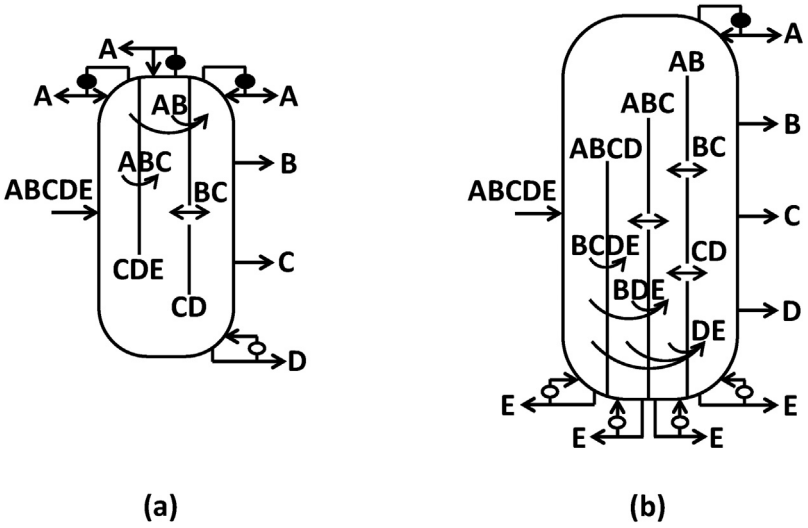

Fig. 21 – Easy-to-operate FTC DWCs using AMR dividing walls for (a) quaternary feed separation; (b) five-component feed separation.

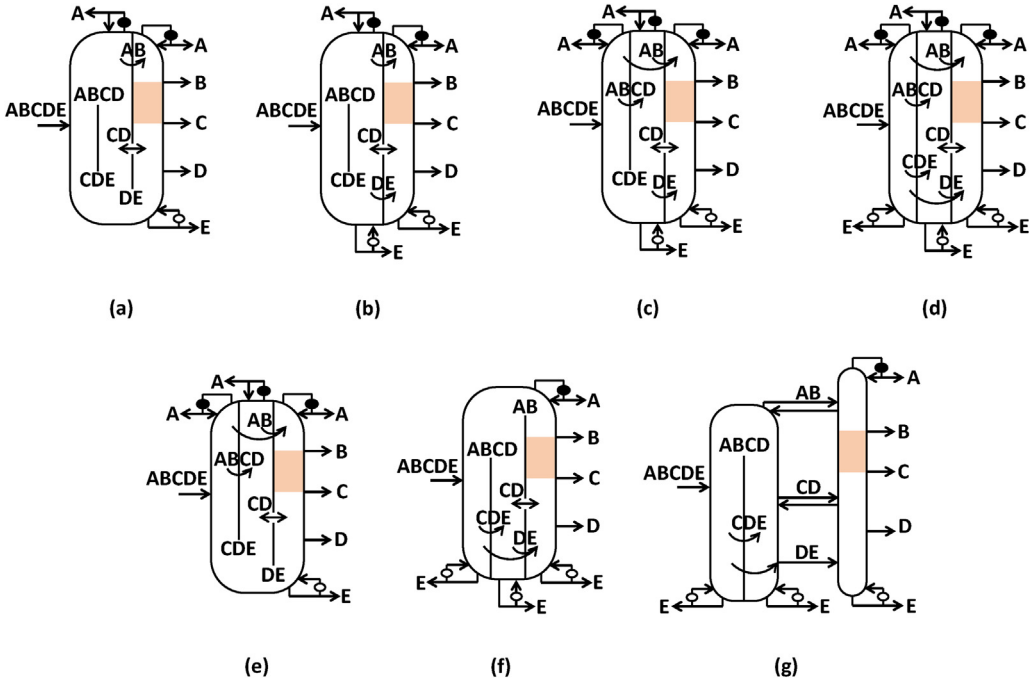

Fig. 22 – (a–d) Some possible DWCs for the HMP configuration of Fig. 15b with increasing operability. The DWCs in (c) and (d) are fully operable since each parallel zone has at least one reboiler and/or condenser; (e and f) fully operable DWC versions that require the least total number of heat exchangers as well as ALT streams; (g) an operable version of the HMP configuration that uses two column shells.

in Fig. 22, then the configuration is equivalent to the HMP configuration of Fig. 15b.

It is informative to compare the five-component FTC DWC of Fig. 21b with some of the DWCs derived from the HMP configuration, which are illustrated in Fig. 22. Notice from Fig. 21b that the simplest operable DWC version for the five-component FTC configuration of Fig. 4 has a total of three partitions and nine submixtures. On the other hand, the single-shell operable DWCs of Fig. 22e and f, which have the same V_{tot}^{min} as the FTC configuration under various feed conditions as discussed earlier, require only two vertical partitions and five submixtures. The structural simplicity associated with these DWC versions is inherited from the original HMP configuration of Fig. 15a and b.

Finally, we observe that due to potential benefits, we have seen an increase in the use of DWCs for industrial applications. According to Dejanović et al. (2010), the number of DWCs installed has passed over 100 in 2009. In particular, BASF only operated about 25 DWCs in 2002 (Schultz et al., 2002), 50 in 2006 (Kenig et al., 2006), and 70 in the year of 2014 (Górak and Olujić, 2014). Industrial applications of DWCs at other companies such as BP, Sasol, Krupp Uhde, and Bayer have also been reported (Górak and Olujić, 2014; Staak et al., 2014). However, compared to the number of conventional distillation columns currently in operation in the chemical and petrochemical industry, this number is still quite minuscule. Also, almost all industrial implementations of DWC have been for separations into three product streams (Halvorsen and Skogestad,

2011). So far, the only reported quaternary DWC for industrial use is a Kaibel column built by BASF which still uses only one partition (Olujić et al., 2009). This DWC incorporates complex internal design together with various proprietary reflux splitters and liquid distributors for controllable operation. And we have not yet seen any industrial implementation of DWC with multiple unextended partitions for ≥5-component separations. We hope that with the recent progress described here for DWCs and the availability of an array of easy-to-operate DWC alternatives, we will see an accelerated rise in the use of DWCs, leading to the ultimate form of PI in multicomponent distillation.

7. Conclusion

Process Intensification has gained tremendous attention, yet despite this increasing interest, the full landscape of PI remains unexploited in the area of multicomponent distillation. Over the past decades, several new methodologies have been developed that allow us to synthesize compact, easy-to-operate, energy efficient and cost-effective multicomponent distillation configurations. All these strategies fall under the category of PI. In this review article, as shown in the PI roadmap of Fig. 1, we piece these PI strategies together in an organized manner and, for the first time, propose a systematic, multi-layer approach for PI in multicomponent distillation.

This approach starts from the complete enumeration of all possible basic regular-column configurations using the SA method (Shah and Agrawal, 2010). Once a basic configuration is identified, thermal couplings can be systematically introduced to synthesize TC derivatives. Strategic replacement of submixture reboilers and/or condensers with thermal couplings forms the foundation to all subsequent PI strategies. Using state-of-art global optimization algorithms (Nallasivam et al., 2016), the best performing TC derivative in terms of heat duty and utility (temperature-level) cost can be identified. Next, two independent PI strategies – column section rearrangement (Agrawal, 1999) and elimination of intercolumn vapor transfer in a thermal coupling using ALT stream to provide one-way liquid transfer (Agrawal, 2000b) – can be implemented to reduce the operational difficulty of a TC configuration without affecting its heat duty benefit. For a given TC configuration, systematic utilization of these PI strategies leads to a series of new thermodynamically equivalent configurations, many of which are easy-to-operate and cost-effective. These two strategies also play an essential role in constructing subsequent layers of PI.

By converting thermal coupling links with ALT streams, operable multi-effect distillation becomes a feasible and attractive option for TC columns for the first time (Agrawal, 2000a). Independently, we also discovered a simple, but powerful rule recently about simultaneous heat and mass integration (Jiang et al., 2018a) for a special set of CTC configurations. We show that for these CTC configurations, heat and mass integration only between final pure product ends is sufficient to offer maximum heat duty savings. This forms a new class of simple, easy-to-build HMP configurations that require the least number of column sections among all configurations in the search space to achieve the same heat duty benefits as the FTC configuration under many feed conditions.

In the last layer, we integrate the PI strategies discussed above in the MTA method to successfully synthesize all possible DWCs associated with any TC configuration (Madenoor Ramapriya et al., 2018b) and solve the longstanding operational challenge that hinders DWCs from being implemented in large scale in industry (Madenoor Ramapriya et al., 2014, 2018c). Some of these DWC arrangements use the unique AMR dividing wall (Agrawal and Madenoor Ramapriya, 2016), whereby a liquid submixture stream is transferred from one side of the dividing wall to an intermediate location on the other side of the wall, and the dividing wall terminates either at the top or the bottom of the column shell with an associated condenser or a reboiler. The AMR dividing wall is an enabler for ease of operation of a large number of DWC arrangements. The discovery of compact, energy efficient, cost-effective multicomponent distillation systems containing fully operable DWCs and using 1 to $n-2$ column shells is a classic example of PI at its best.

Once process synthesis phase is complete, process engineers are left with a handful of intensified flowsheets to choose from. To make the proper choice of the best flowsheet design and its optimal operating conditions and control strategies, they need to perform more rigorous economic and process dynamics analyses in the process design phase (Skogestad, 1997; Sakizlis et al., 2004; Serra et al., 2003, 2000; Ricardez-Sandoval et al., 2010; Dwivedi et al., 2012; Adrian et al., 2004). In particular, it is important to understand how the distillation system would respond to disturbances as well as uncertainties under normal and abnormal operation settings (Ruiz et al., 1988; Bansal et al., 2002, 2000; Trainor et al., 2013; Sánchez-Sánchez and Ricardez-Sandoval, 2013; Mohideen et al., 1996).

Overall, the systematic, multi-layer PI approach opens the door to the great opportunities for PI in multicomponent distillation. We hope that the analyses and examples discussed here inspire and guide industrial practitioners towards synthesizing and building novel and attractive intensified multicomponent distillation systems.

Acknowledgments

The information, data, or work presented herein was funded in part by the Office of Energy Efficiency and Renewable Energy (EERE), U.S. Department of Energy, under Award Number DE-EE0005768. RA also thanks all his graduate students and Professor Mohit Tawarmalani for their help in the development of several concepts described here.

References

Abdul Mutalib, M., Smith, R., 1998. Operation and control of dividing wall distillation columns: Part 1: Degrees of freedom and dynamic simulation. Chem. Eng. Res. Des. 76, 308–318, http://dx.doi.org/10.1205/026387698524956, Techno-economic analysis.

Adrian, T., Schoenmakers, H., Boll, M., 2004. Model predictive control of integrated unit operations: control of a divided wall column. Chem. Eng. Process.: Process Intensif. 43, 347–355, http://dx.doi.org/10.1016/S0255-2701(03)00114-4.

Agrawal, R., 1996. Synthesis of distillation column configurations for a multicomponent separation. Ind. Eng. Chem. Res. 35, 1059–1071, http://dx.doi.org/10.1021/ie950323h.

Agrawal, R., 1999. More operable fully thermally coupled distillation column configurations for multicomponent distillation. Chem. Eng. Res. Des. 77, 543–553, http://dx.doi.org/10.1205/026387699526449.

Agrawal, R., 2000a. Multieffect distillation for thermally coupled configurations. AIChE J. 46, 2211–2224, http://dx.doi.org/10.1002/aic.690461113.

Agrawal, R., 2000b. Thermally coupled distillation with reduced number of intercolumn vapor transfers. AIChE J. 46, 2198–2210, http://dx.doi.org/10.1002/aic.690461112.
Agrawal, R., 2001. Multicomponent distillation columns with partitions and multiple reboilers and condensers. Ind. Eng. Chem. Res. 40, 4258–4266, http://dx.doi.org/10.1021/ie000315n.
Agrawal, R., 2003. Synthesis of multicomponent distillation column configurations. AIChE J. 49, 379–401, http://dx.doi.org/10.1002/aic.690490210.
Agrawal, R., Fidkowski, Z.T., 1998a. Are thermally coupled distillation columns always thermodynamically more efficient for ternary distillations? Ind. Eng. Chem. Res. 37, 3444–3454, http://dx.doi.org/10.1021/ie980062m.
Agrawal, R., Fidkowski, Z.T., 1998b. More operable arrangements of fully thermally coupled distillation columns. AIChE J. 44, 2565–2568, http://dx.doi.org/10.1002/aic.690441124.
Agrawal, R., Fidkowski, Z.T., 1999. New thermally coupled schemes for ternary distillation. AIChE J. 45, 485–496, http://dx.doi.org/10.1002/aic.690450306.
Agrawal, R., Madenoor Ramapriya, G., 2016. Multicomponent dividing wall columns. US Patent 9504934B2.
Agrawal, R., Yee, T.F., 1994. Heat pumps for thermally linked distillation columns: an exercise for argon production from air. Ind. Eng. Chem. Res. 33, 2717–2730, http://dx.doi.org/10.1021/ie00035a023.
Amminudin, K., Smith, R., Thong, D.C., Towler, G., 2001. Design and optimization of fully thermally coupled distillation columns: Part 1: Preliminary design and optimization methodology. Chem. Eng. Res. Des. 79, 701–715, http://dx.doi.org/10.1205/026387601753192028.
Annakou, O., Mizsey, P., 1996. Rigorous comparative study of energy-integrated distillation schemes. Ind. Eng. Chem. Res. 35, 1877–1885, http://dx.doi.org/10.1021/ie950445+.
Bagajewicz, M., Ji, S., 2001. Rigorous procedure for the design of conventional atmospheric crude fractionation units. Part I: Targeting. Ind. Eng. Chem. Res. 40, 617–626, http://dx.doi.org/10.1021/ie000302+.
Bansal, V., Perkins, J., Pistikopoulos, E., Ross, R., van Schijndel, J., 2000. Simultaneous design and control optimisation under uncertainty. Comput. Chem. Eng. 24, 261–266, http://dx.doi.org/10.1016/S0098-1354(00)00475-0.
Bansal, V., Perkins, J.D., Pistikopoulos, E.N., 2002. A case study in simultaneous design and control using rigorous, mixed-integer dynamic optimization models. Ind. Eng. Chem. Res. 41, 760–778, http://dx.doi.org/10.1021/ie010156n.
Brugma, A.J., 1942. Process and device for fractional distillation of liquid mixtures, more particularly petroleum. US Patent 2295256A.
Caballero, J.A., Grossmann, I.E., 2001. Generalized disjunctive programming model for the optimal synthesis of thermally linked distillation columns. Ind. Eng. Chem. Res. 40, 2260–2274, http://dx.doi.org/10.1021/ie000761a.
Caballero, J.A., Grossmann, I.E., 2003. Thermodynamically equivalent configurations for thermally coupled distillation. AIChE J. 49, 2864–2884, http://dx.doi.org/10.1002/aic.690491118.
Caballero, J.A., Grossmann, I.E., 2004. Design of distillation sequences: from conventional to fully thermally coupled distillation systems. Comput. Chem. Eng. 28, 2307–2329, http://dx.doi.org/10.1016/j.compchemeng.2004.04.010.
Caballero, J.A., Grossmann, I.E., 2006. Structural considerations and modeling in the synthesis of heat-integrated-thermally coupled distillation sequences. Ind. Eng. Chem. Res. 45, 8454–8474, http://dx.doi.org/10.1021/ie060030w.
Caballero, J.A., Grossmann, I.E., 2013. Synthesis of complex thermally coupled distillation systems including divided wall columns. AIChE J. 59, 1139–1159, http://dx.doi.org/10.1002/aic.13912.
Cahn, R.P., Di Miceli, A.G., Di Miceli, E., 1962. Separation of multicomponent mixture in single tower. US Patent 3058893A.
Carlberg, N.A., Westerberg, A.W., 1989. Temperature-heat diagrams for complex columns. 2. Underwood's method for side strippers and enrichers. Ind. Eng. Chem. Res. 28, 1379–1386, http://dx.doi.org/10.1021/ie00093a017.
Cheng, H.C., Luyben, W.L., 1985. Heat-integrated distillation columns for ternary separations. Ind. Eng. Chem. Process Des. Dev. 24, 707–713, http://dx.doi.org/10.1021/i200030a031.
Christiansen, A.C., Skogestad, S., Lien, K., 1997. Complex distillation arrangements: extending the Petlyuk ideas. Comput. Chem. Eng. 21, S237–S242, http://dx.doi.org/10.1016/S0098-1354(97)87508-4, Supplement to Computers and Chemical Engineering.
Dejanović, I., Matijašević, L., Olujić, Z., 2010. Dividing wall column – a breakthrough towards sustainable distilling. Chem. Eng. Process.: Process Intensif. 49, 559–580, http://dx.doi.org/10.1016/j.cep.2010.04.001.
Ding, S.S., Luyben, W.L., 1990. Control of a heat-integrated complex distillation configuration. Ind. Eng. Chem. Res. 29, 1240–1249, http://dx.doi.org/10.1021/ie00103a024.
Dwivedi, D., Strandberg, J.P., Halvorsen, I.J., Preisig, H.A., Skogestad, S., 2012. Active vapor split control for dividing-wall columns. Ind. Eng. Chem. Res. 51, 15176–15183, http://dx.doi.org/10.1021/ie3014346.
Emtir, M., Rév, E., Fonyó, Z., 2001. Rigorous simulation of energy integrated and thermally coupled distillation schemes for ternary mixture. Appl. Therm. Eng. 21, 1299–1317, http://dx.doi.org/10.1016/S1359-4311(01)00017-5.
Engelien, H.K., Skogestad, S., 2005. Minimum energy diagrams for multieffect distillation arrangements. AIChE J. 51, 1714–1725, http://dx.doi.org/10.1002/aic.10453.
Fidkowski, Z., Krolikowski, L., 1986. Thermally coupled system of distillation columns: optimization procedure. AIChE J. 32, 537–546, http://dx.doi.org/10.1002/aic.690320403.
Fidkowski, Z., Krolikowski, L., 1987. Minimum energy requirements of thermally coupled distillation systems. AIChE J. 33, 643–653, http://dx.doi.org/10.1002/aic.690330412.
Fidkowski, Z.T., 2006. Distillation configurations and their energy requirements. AIChE J. 52, 2098–2106, http://dx.doi.org/10.1002/aic.10803.
Fidkowski, Z.T., Agrawal, R., 2001. Multicomponent thermally coupled systems of distillation columns at minimum reflux. AIChE J. 47, 2713–2724, http://dx.doi.org/10.1002/aic.690471211.
Flores, O.A., Cárdenas, J.C., Hernández, S., Rico-Ramírez, V., 2003. Thermodynamic analysis of thermally coupled distillation sequences. Ind. Eng. Chem. Res. 42, 5940–5945, http://dx.doi.org/10.1021/ie034011n.
Giridhar, A., Agrawal, R., 2010a. Synthesis of distillation configurations: I. Characteristics of a good search space. Comput. Chem. Eng. 34, 73–83, http://dx.doi.org/10.1016/j.compchemeng.2009.05.003.
Giridhar, A., Agrawal, R., 2010b. Synthesis of distillation configurations. II. A search formulation for basic configurations. Comput. Chem. Eng. 34, 84–95, http://dx.doi.org/10.1016/j.compchemeng.2009.05.004.
Glinos, K., Malone, M.F., 1985. Minimum vapor flows in a distillation column with a sidestream stripper. Ind. Eng. Chem. Process Des. Dev. 24, 1087–1090, http://dx.doi.org/10.1021/i200031a032.
Glinos, K.N., Nikolaides, I.P., Malone, M.F., 1986. New complex column arrangements for ideal distillation. Ind. Eng. Chem. Process Des. Dev. 25, 694–699, http://dx.doi.org/10.1021/i200034a016.
Górak, A., Olujić, Z., 2014. Distillation: Fundamentals and Principles. Elsevier Inc.
Halvorsen, I.J., Skogestad, S., 2003. Minimum energy consumption in multicomponent distillation. 3. More than three products and generalized Petlyuk arrangements. Ind. Eng. Chem. Res. 42, 616–629, http://dx.doi.org/10.1021/ie0108651.
Halvorsen, I.J., Skogestad, S., 2011. Energy efficient distillation. J. Nat. Gas Sci. Eng. 3, 571–580, http://dx.doi.org/10.1016/j.jngse.2011.06.002.
Hernández, S., Pereira-Pech, S., Jiménez, A., Rico-Ramírez, V., 2003. Energy efficiency of an indirect thermally coupled

distillation sequence. Can. J. Chem. Eng. 81, 1087–1091, http://dx.doi.org/10.1002/cjce.5450810522.
Humphrey, J.L., 1992. Separation technologies: an opportunity for energy savings. Chem. Eng. Prog. 88, 32–42.
Ivakpour, J., Kasiri, N., 2009. Synthesis of distillation column sequences for nonsharp separations. Ind. Eng. Chem. Res. 48, 8635–8649, http://dx.doi.org/10.1021/ie802013r.
Jiang, Z., Madenoor Ramapriya, G., Tawarmalani, M., Agrawal, R., 2018a. Minimum energy of multicomponent distillation systems using minimum additional heat and mass integration sections. AIChE J. 64, 3410–3418, http://dx.doi.org/10.1002/aic.16189.
Jiang, Z., Madenoor Ramapriya, G., Tawarmalani, M., Agrawal, R., 2018b. Process intensification in multicomponent distillation. Chem. Eng. Trans. 69, 841–846, http://dx.doi.org/10.3303/CET1869141.
Jiang, Z., Agrawal, R., 2019. Global optimization of multicomponent distillation configurations: global minimization of total cost for multicomponent mixture separations. Comput. Chem. Eng. 126, 249–262, http://dx.doi.org/10.1016/j.compchemeng.2019.04.009.
Kaibel, G., 1987. Distillation columns with vertical partitions. Chem. Eng. Technol. 10, 92–98, http://dx.doi.org/10.1002/ceat.270100112.
Kenig, E., Müller, I., Großmann, C., Geißler, E., Kaibel, G., Schoenmakers, H., 2006. Trennwandkolonnen: Entwicklungsstand und perspektiven. Chem. Ing. Tech. 78, 1281–1282, http://dx.doi.org/10.1002/cite.200650379.
Kolbe, B., Wenzel, S., 2004. Novel distillation concepts using one-shell columns. Chem. Eng. Process.: Process Intensif. 43, 339–346, http://dx.doi.org/10.1016/S0255-2701(03)00133-8, Special Issue on Distillation and Absorption.
Lestak, F., Collins, C., 1997. Advanced distillation saves energy and capital. Chem. Eng. 104, 72–76.
Liebmann, K., Dhole, V., 1995. Integrated crude distillation design. Comput. Chem. Eng. 19, 119–124, http://dx.doi.org/10.1016/0098-1354(95)87025-3.
Madenoor Ramapriya, G., Selvarajah, A., Jimenez Cucaita, L.E., Huff, J., Tawarmalani, M., Agrawal, R., 2018a. Short-cut methods versus rigorous methods for performance-evaluation of distillation configurations. Ind. Eng. Chem. Res. 57, 7726–7731, http://dx.doi.org/10.1021/acs.iecr.7b05214.
Madenoor Ramapriya, G., Shenvi, A.A., Tawarmalani, M., Agrawal, R., 2015. A new framework for combining a condenser and reboiler in a configuration to consolidate distillation columns. Ind. Eng. Chem. Res. 54, 10449–10464, http://dx.doi.org/10.1021/acs.iecr.5b01701.
Madenoor Ramapriya, G., Tawarmalani, M., Agrawal, R., 2014. Thermal coupling links to liquid-only transfer streams: a path for new dividing wall columns. AIChE J. 60, 2949–2961, http://dx.doi.org/10.1002/aic.14468.
Madenoor Ramapriya, G., Tawarmalani, M., Agrawal, R., 2016. Thermal coupling links to liquid-only transfer streams: an enumeration method for new FTC dividing wall columns. AIChE J. 62, 1200–1211, http://dx.doi.org/10.1002/aic.15053.
Madenoor Ramapriya, G., Tawarmalani, M., Agrawal, R., 2018b. A systematic method to synthesize all dividing wall columns for n-component separation: Part 1. AIChE J. 64, 649–659, http://dx.doi.org/10.1002/aic.15964.
Madenoor Ramapriya, G., Tawarmalani, M., Agrawal, R., 2018c. A systematic method to synthesize all dividing wall columns for *n*-component separation: Part 2. AIChE J. 64, 660–672, http://dx.doi.org/10.1002/aic.15963.
Mizsey, P., Hau, N., Benko, N., Kalmar, I., Fonyó, Z., 1998. Process control for energy integrated distillation schemes. Comput. Chem. Eng. 22, S427–S434, http://dx.doi.org/10.1016/S0098-1354(98)00084-2.
Mohideen, M.J., Perkins, J.D., Pistikopoulos, E.N., 1996. Optimal design of dynamic systems under uncertainty. AIChE J. 42, 2251–2272, http://dx.doi.org/10.1002/aic.690420814.
Monro, D., 1938. Fractionating apparatus and method of fractionation. US Patent 2134882.
Nallasivam, U., Shah, V.H., Shenvi, A.A., Huff, J., Tawarmalani, M., Agrawal, R., 2016. Global optimization of multicomponent distillation configurations: 2. Enumeration based global minimization algorithm. AIChE J. 62, 2071–2086, http://dx.doi.org/10.1002/aic.15204.
Nallasivam, U., Shah, V.H., Shenvi, A.A., Tawarmalani, M., Agrawal, R., 2013. Global optimization of multicomponent distillation configurations: 1. Need for a reliable global optimization algorithm. AIChE J. 59, 971–981, http://dx.doi.org/10.1002/aic.13875.
Ognisty, T., Manley, D., 1998. Partitioned distillation column. US Patent 5755933.
Olujić, Z., Jodecke, M., Shilkin, A., Schuch, G., Kaibel, B., 2009. Equipment improvement trends in distillation. Chem. Eng. Process.: Process Intensif. 48, 1089–1104, http://dx.doi.org/10.1016/j.cep.2009.03.004.
Petlyuk, F., Platonov, V., Slavinskii, D., 1965. Thermodynamically optimal method for separating multicomponent mixtures. Int. Chem. Eng. 5, 555–561.
Ponce-Ortega, J.M., Al-Thubaiti, M.M., El-Halwagi, M.M., 2012. Process intensification: new understanding and systematic approach. Chem. Eng. Process.: Process Intensif. 53, 63–75, http://dx.doi.org/10.1016/j.cep.2011.12.010.
Ramshaw, C., 1995. The incentive for process intensification. In: 1st Intl. Conf. Proc. Intensif. for Chem. Ind., London.
Reay, D.G., Ramshaw, C., Harvey, A., 2013. Process intensification engineering for efficiency, sustainability and flexibility. In: Isotopes in Organic Chemistry, 2nd ed. Elsevier/BH, Amsterdam; Boston.
Rév, E., Emtir, M., Szitkai, Z., Mizsey, P., Fonyó, Z., 2001. Energy savings of integrated and coupled distillation systems. Comput. Chem. Eng. 25, 119–140, http://dx.doi.org/10.1016/S0098-1354(00)00643-8.
Ricardez-Sandoval, L.A., Budman, H.M., Douglas, P.L., 2010. Simultaneous design and control: a new approach and comparisons with existing methodologies. Ind. Eng. Chem. Res. 49, 2822–2833, http://dx.doi.org/10.1021/ie9010707.
Rong, B.G., Kraslawski, A., Turunen, I., 2003. Synthesis of heat-integrated thermally coupled distillation systems for multicomponent separations. Ind. Eng. Chem. Res. 42, 4329–4339, http://dx.doi.org/10.1021/ie030302k.
Ruiz, C., Cameron, I., Gani, R., 1988. A generalized dynamic model for distillation columns – III. Study of startup operations. Comput. Chem. Eng. 12, 1–14, http://dx.doi.org/10.1016/0098-1354(88)85001-4.
Sakizlis, V., Perkins, J.D., Pistikopoulos, E.N., 2004. Recent advances in optimization-based simultaneous process and control design. Comput. Chem. Eng. 28, 2069–2086.
Sánchez-Sánchez, K., Ricardez-Sandoval, L., 2013. Simultaneous process synthesis and control design under uncertainty: a worst-case performance approach. AIChE J. 59, 2497–2514, http://dx.doi.org/10.1002/aic.14040.
Sargent, R., Gaminibandara, K., 1976. Optimal design of plate distillation columns. In: Dixon, L. (Ed.), Optimization in Action, Conference on Optimization in Action (1975: University of Bristol). Academic Press, New York.
Schultz, M., Stewart, D., Harris, J., Rosenblum, S., Shakur, M., O'Brien, D., 2002. Reduce costs with dividing-wall columns. Chem. Eng. Prog. 98, 64–71.
Segovia-Hernández, J.G., Bonilla-Petriciolet, A., 2016. Process Intensification in Chemical Engineering – Design Optimization and Control. Springer.
Serra, M., Espuña, A., Puigjaner, L., 2003. Controllability of different multicomponent distillation arrangements. Ind. Eng. Chem. Res. 42, 1773–1782.
Serra, M., Perrier, M., Espuña, A., Puigjaner, L., 2000. Study of the divided wall column controllability: influence of design and operation. Comput. Chem. Eng. 24, 901–907, http://dx.doi.org/10.1016/S0098-1354(00)80004-6.
Shah, V.H., Agrawal, R., 2010. A matrix method for multicomponent distillation sequences. AIChE J. 56, 1759–1775, http://dx.doi.org/10.1002/aic.12118.

Shah, V.H., Agrawal, R., 2011. Are all thermal coupling links between multicomponent distillation columns useful from an energy perspective? Ind. Eng. Chem. Res. 50, 1770–1777, http://dx.doi.org/10.1021/ie101768c.

Shenvi, A.A., Shah, V.H., Agrawal, R., 2013. New multicomponent distillation configurations with simultaneous heat and mass integration. AIChE J. 59, 272–282, http://dx.doi.org/10.1002/aic.13971.

Sholl, D.S., Lively, R.P., 2016. Seven chemical separations to change the world. Nature 532, 435–437.

Skogestad, S., 1997. Dynamics and control of distillation columns: a tutorial introduction. Chem. Eng. Res. Des. 75, 539–562, Distillation.

Smith, R., Linnhoff, B., 1988. The design of separators in the context of overall processes. Chem. Eng. Res. Des. 66, 195–228.

Staak, D., Grutzner, T., Schwegler, B., Roederer, D., 2014. Dividing wall column for industrial multi purpose use. Chem. Eng. Process.: Process Intensif. 75, 48–57.

Stankiewicz, A., Moulijn, J., 2000. Process intensification: transforming chemical engineering. Chem. Eng. Prog. 96 http://search.proquest.com/docview/221526920/.

Tawarmalani, M., Sahinidis, N.V., 2005. A polyhedral branch-and-cut approach to global optimization. Math. Program. 103, 225–249.

Thompson, R.W., King, C.J., 1972. Systematic synthesis of separation schemes. AIChE J. 18, 941–948, http://dx.doi.org/10.1002/aic.690180510.

Trainor, M., Giannakeas, V., Kiss, C., Ricardez-Sandoval, L., 2013. Optimal process and control design under uncertainty: a methodology with robust feasibility and stability analyses. Chem. Eng. Sci. 104, 1065–1080, http://dx.doi.org/10.1016/j.ces.2013.10.017.

Triantafyllou, C., Smith, R., 1992. Design and optimisation of fully thermally coupled distillation columns. Chem. Eng. Res. Des. 70, 118–132.

Underwood, A.J.V., 1949. Fractional distillation of multicomponent mixtures. Ind. Eng. Chem. 41, 2844–2847, http://dx.doi.org/10.1021/ie50480a044.

Van Gerven, T., Stankiewicz, A., 2009. Structure, energy, synergy, time – the fundamentals of process intensification. Ind. Eng. Chem. Res. 48, 2465–2474, http://dx.doi.org/10.1021/ie801501y.

Wankat, P.C., 1993. Multieffect distillation processes. Ind. Eng. Chem. Res. 32, 894–905, http://dx.doi.org/10.1021/ie00017a017.

Wolff, E.A., Skogestad, S., 1995. Operation of integrated three-product (Petlyuk) distillation columns. Ind. Eng. Chem. Res. 34, 2094–2103, http://dx.doi.org/10.1021/ie00045a018.

Wright, R.O., 1949. Fractionation apparatus. US Patent 2471134A.